Supplemental Materials

Inhibition of 2-Hydroxyglutarate Elicits Metabolic-reprograming and Mutant IDH1 Glioma Immunity in Mice.

Padma Kadiyala[1,2], Stephen V. Carney[1,2], Jessica C. Gauss[1,2], Maria B. Garcia-Fabiani[1,2], Santiago Haase[1,2], Mahmoud S. Alghamri[1,2], Felipe J. Núñez[1,2,#], Yayuan Liu[3], Minzhi Yu[3], Ayman Taher[1,2], Fernando M. Nunez[1,2], Dan Li[3], Marta B. Edwards[1], Celina G. Kleer[5], Henry Appelman[5], Yilun Sun[6,7], Lili Zhao,[7] James J. Moon[3,4,8], Anna Schwendeman[3,4], Pedro R. Lowenstein[1,2,4] and Maria G. Castro[1,2,4]*

Affiliations:

[1] Department of Neurosurgery, University of Michigan Medical School, Ann Arbor, MI 48109, USA

[2] Department of Cell and Developmental Biology, University of Michigan Medical School, Ann Arbor, MI 48109, USA

[3] Department of Pharmaceutical Sciences, University of Michigan, Ann Arbor, MI 48109, USA

[4] Biointerfaces Institute, University of Michigan Medical School, Ann Arbor, MI 48109, USA

[5] Department of Pathology, University of Michigan Medical School, Ann Arbor, MI 48109, USA

[6]Department of Radiation Oncology, University of Michigan Medical School, Ann Arbor, MI 48109, USA

[7]Department of Biostatistics, University of Michigan Medical School, Ann Arbor, MI 48109, USA

[8]Department of Biomedical Engineering, University of Michigan, Ann Arbor, MI 48109, USA

Current Address: Leloir Institute Foundation, Buenos Aires, Argentina.

[*]**Corresponding Author:** Email: mariacas@med.umich.edu

Key Words: Mutant IDH1, genetically engineered glioma models, IDH1-R132H Inhibitors, Immunotherapy.

Supplementary Methods

Reagents

DMEM-F12, DMEM RPMI- 1650, FBS, PBS, N2, and B27 supplements and penicillin-streptomycin were purchased from GIBCO, Life Technologies. Epidermal growth factor (EGF) and fibroblast growth factor (FGF) were purchased from Peprotech. Anti-mouse CD45, CD11c, B220, F4/80, CD206, CD3, CD4, CD8, CD25, CD80, CD86, MHC II, CD44, CD62L, Gr1, CD11b, and PDL1 antibodies for flow cytometry analysis were obtained from Biolegend. SIINFEKL tetramers were obtained from MBL International (Supplementary Table 6). For immunohistochemistry, anti-mouse MBP and GFAP primary antibody were purchased from Millipore; anti-mouse Cleaved Caspase 3, and PD-L1 were purchased from Cell Signaling; anti-mouse Ki-67 and Calreticulin were purchased from Abcam; and anti-mouse CD8 was purchased from Cedarlane (Supplementary Table 7). Secondary antibodies for immunohistochemistry were purchased from Thermofisher and Dako (Supplementary Table 8). AGI-5198 compound was purchased from Amatek Chemical Co; Temozolomide was purchased from Selleckchem; and Anti mouse PD-L1 for in vivo studies was purchased from BioXcell (Supplementary Table 9).

Cell Culture

Mouse wtIDH neurospheres and mouse mIDH1 neurospheres were grown in DMEM-F12 media supplemented with 100 units/mL Penicillin- Streptomycin, 1x B-27, 1x N-2, 100ug/mL Normocin, 20ng/mL hFGF and 20ng/mL hEGF (NSC media). Mouse mIDH1-OVA neurospheres were grown in NSC media supplemented with 100 units/mL puromycin. Human SJGBM2-Wt neurospheres were grown in NSC media. Human SJGBM2-mIDH1 neurospheres were grown in

NSC media supplemented with 800µg/mL G418. Human MGG119 neurosphere cell were grown in Neurobasal media supplemented with 100 units/mL Penicillin- Streptomycin, 1x B-27, 1x N-2, 100ug/mL Normocin, 20ng/mL hFGF and 20ng/mL hEGF. Human SF10602 cells were grown in Neurocult NS-A media supplemented with 100units/mL Penicilin-Streptomycin, 1x B27, 1x N-2, 1x Sodium Pyruvate, 20ng/µL hFGF, 20ng/µL hEGF, and 20ng/µL PDGF-AA. SJGBM2 glioma cells were shared by Children's Oncology Group (COG) Repository, Health Science Center, Texas Tech University (1). MGG119 glioma cells were shared by Dr. Daniel P. Cahill laboratory, Harvard Medical School (2). SF10602 glioma cells were shared by Dr. Joseph Costello's laboratory, UCSF (3). Neurospheres and cells were dissociated with Accutase detachment reagent when they had to passaged. Cells were maintained in a humidified incubator at 95% air/5% CO2 at 37°C and passaged every 2-4 days.

Animal Strains

Six to eight-week-old female C57BL/6 and CD8 knockout mice were purchased from Jackson Laboratory (Bar Harbor, ME) and were housed in pathogen free conditions at the University of Michigan. The mice in the untreated groups in the tumor rechallenge studies (Fig 2F, 4C, 8) were 6-8 weeks old at the time of tumor implantation and they were not age matched with the mice that were long term survivors from the treatment group.

Clonogenic Assay

Mouse and human (SJGBM2:wtIDH1, MGG119: mIDH1) glioma cells were seeded at density of 1.0 x 10^6 cells into 25-cm^2 flasks containing DMEM medium supplemented with 10% fetal bovine serum, and 100U/mL Penicillin-Streptomycin. Mouse cells were treated with 1.5 µM

AGI-5198; human glioma cells were treated with 5μM AGI-5198. DMSO was utilized as vehicle control. Cells were maintained in culture for ten days, media containing AGI-5198 or vehicle control was replaced every 2 days. On day ten, mouse and human glioma cells were plated (10×10^4 cells/well) into 6 well plates in DMEM medium supplemented with 10% fetal bovine serum and 100U/mL Penicillin-Streptomycin. After 24 hours, cells were treated with escalating doses of radiation (Mouse cells: 0, 2, 4, and 8 Gy; Human cells: 0, 5, 10, and 20Gy). Cells were then trypsinized, serially diluted and seeded (cell numbers ranging from 100 to 2000 cells per cell type were plated depending on the radiation dose) in triplicates into 6-well plates. Cells were maintained in a humidified incubator at 95% air/5% CO2 at 37°C for 10 days. Once the colony formation was observed, plates were washed with PBS and cell colonies were stained with 0.25% crystal violet. Colonies were counted using a bright field microscope. The survival fraction was calculated relative to DMSO vehicle control.

DAMPs Measurement

Mouse mIDH1 neurospheres and MGG119 glioma cells were seeded at density of 1.0 x 10^6 cells into 25-cm^2 flasks containing NSC media. Mouse cells were treated with 1.5 μM AGI-5198; human glioma cells were treated with 5μM AGI-5198. DMSO was utilized as vehicle control. Cells were maintained in culture for ten days, media containing AGI-5198 or vehicle control was replaced every 2 days. On day ten, mouse and human glioma cells were plated (10×10^4 cells/well) into 6 well plates in NSC media. After 24 hours, mouse neurospheres and human glioma cells were treated with 3Gy and 10Gy radiation respectively. After an additional 24 hrs, mouse neurospheres and human glioma cells were treated with 1.5μM and 5μM AGI-5198 or DMSO vehicle control respectively. Release of DAMPs was assessed 72 hours post radiation and

48 hours post AGI-5198 treatment. Neurospheres were collected, dissociated with Accutase and stained with anti-Calreticulin antibody (1:50) in PBS containing 2% FCS (flow buffer) for 25 minutes at 4°C. Cells were then washed three times with flow buffer and the fluorescence of the samples was read on a BD FACS ARIA SORP (BD Bioscience) using the 647 laser (APC setting). Data were analyzed with Flowjo v.10 Software. Levels of HMGB-1, IL-1α, and IL-6 in the cultures' supernatants was measured by ELISA according to manufacturer's instructions (R&D) at the Cancer Center Immunology Core, University of Michigan. Levels of ATP in the cultures' supernatants was measured by ENLITEN® ATP Assay according to manufacturer's instructions (Promega).

Determination of 2-HG in brain samples.

2HG concentration in the tumor microenvironment of untreated normal mice, wtIDH1 and mIDH1 glioma bearing mice; and mIDH1 glioma bearing mice treated with AGI-5198 was assessed by liquid chromatography-mass spectrometry (UPLC-MS). AGI-5198 (40 mg/kg) was injected intraperitonially (i.p) into mice bearing mIDH1 glioma at 7, 9, 11, 14, 16, 18, 21, 23, 25 days post tumor cell implantation (dpi). Brains from untreated control mice, wtIDH1 and mIDH1 glioma bearing +/- AGI-5198 treatment were harvested for analysis at 27 dpi. Brain tissue (10-15mg) was mixed with 10 μL of internal standard solution containing 10 μg/mL of 2-HG-D3 (Sigma-Aldrich), and was homogenized in 1 mL of methanol/water (80:20, v/v). The homogenate was centrifuged at 12000 rpm for 10 min at 4 °C, and the supernatant was collected and dried under a stream of nitrogen at 37 °C. Then 160 μL of N-(p-toluenesulfonyl)-L-phenylalanyl chloride (TSPC, 2.5 mM in acetonitrile) and 2 μL of pyridine was added, and the samples were incubated at 37 °C for 20 min to derivatize D-2HG. After derivatization the mixture was dried with

nitrogen at 37 °C and reconstituted in 100 μL of acetonitrile/water (50:50, v/v). The samples were then centrifuged at 12000 RPM for 10 min and the supernatant was collected for quantification. The quantification of derivatized 2-HG was carried out using ultra performance UPLC-MS (Waters ACQUITY system). The mobile phase consisted of deionized water containing 0.1% formic acid (A) and acetonitrile/methanol (1:1, v/v) containing 0.1% formic acid (B). The gradient started from 70% A and maintained for 1 min, changed to 30% A over 3 min and maintained for 2 min, and finally changed back to 70% A over 0.5 min and held for 1.5 min. The flow rate was 0.5 mL/min, and column temperature was set at 40 °C. The analysis was performed on a Waters ACQUITY UPLC HSS T3 column (1.8 μm, 3.0 × 75 mm) with mass detection at 448.17 (-) for derivatized 2-HG, and at 451.19 (-) for derivatized 2-HG-D3.

Intracranial mIDH1 glioma models

Mouse glioma models: We used the Sleeping Beauty (SB) Transposase System to generate genetically engineered immunocompetent wtIDH and mIDH1 mouse models of glioma harboring ATRX and TP53 loss (4). The wtIDH glioma includes genetic lesions in NRASG12V, *Atrx* and *Tp53* knockdown. The mIDH1 glioma model includes genetic lesions in NRASG12V, *Atrx* and *Tp53* knockdown with the addition of IDH1-R132H (4). WtIDH neurospheres derived from SB glioma bearing female mouse and mIDH1 neurospheres derived from SB glioma bearing male mouse were utilized to perform the preclinical experiments in this study (Supplementary Figure 24). Syngeneic tumors were established in C57BL/6 mice by stereotactically injecting 50,000 mIDH1, wtIDH1 or mIDH1-OVA neurospheres into the right striatum using a 22-gauge Hamilton syringe (1 μL over 1 minute) with the following coordinates: +1.00 mm anterior, 2.5 mm lateral, and 3.00 mm deep (4).

Preparation of AGI-5198 Formulation for *in vivo* Studies

Approximately 5 mg AGI-5198 was dissolved in 350 µl ethanol and 350 µL PEG-400, then 300µL water was added to achieve the final volume of 1 ml (final AGI-5198 concentration in the solution was 5 mg/ml). For a 40 mg/kg intraperitoneal dose, ~200µL formulation was injected per mouse.

Radiotherapy

Seven days' post wtIDH1 or mIDH1 tumor cells' implantation, a dose of 2 Gy Irradiation (IR) was administered to mice 5 days a week for two weeks. Mice bearing tumor were placed under a copper Orthovoltage source, their body was shielded with iron collimators to focus the irradiation energy beam to the brain (4, 5). Irradiation treatment was given to mice at the University of Michigan Radiation Oncology Core.

In vivo Cell Cycle Analysis

AGI-5198 (40 mg/kg) or saline was injected i.p into mice bearing mIDH1 glioma at 7, 9, 11, 14, 16, 18, 21, 23, 25 days post tumor cell implantation (dpi). A course of IR (2 Gy) was administered to mice 5 days a week for two weeks starting at 7 dpi (4, 5). At 27 dpi, a dose of 10 mg/kg EdU was i.p injected into mIDH1 tumor bearing mice 3 hours before they were sacrificed. Tumors were dissected and made into single cell suspensions. Immune cells were labeled with CD45 magnetic beads (Miltenyi) following the manufacturer's instructions. After 15 min of incubation at 4 °C, cells were washed and passed through a preconditioned MS column placed in the magnetic field of a suitable MACS Separator. Tumor cells (CD45 negative) were collected and resuspended in flow buffer. Tumor cells were fixed and permeabilized using the BD kit (BD

Biosciences) and stained with pH3-Ser10 (1: 50; Cell Signaling). Click-reaction was performed to detect EdU positive cells following the manufacturer's instructions (ThermoFisher) (4).

Therapeutic Studies in Tumor Bearing Animals

The rationale for AGI-1598+SOC+αPD-L1 treatment schedule used to treat mIDH1 glioma bearing mice in our study is based on the following: (i) Radiation dosing of 2 Gy per day, 5 days a week, for two weeks was adopted from previous work published by our research group in mIDH1 glioma model (4) and others on mouse glioma models (5, 6). A course of IR (2 Gy) was administered to glioma bearing mice 5 days a week for two weeks starting at 7 dpi (4, 5). (ii) It has been well documented that systemic administration of 60 mg/Kg Temozolomide (TMZ) to mice bearing glioma every other day for three weeks is well tolerated with no toxicity(7), thus we decided to treat mIDH1 glioma bearing mice with 60 mg/kg TMZ. TMZ was administered to mice i.p. on days 8, 10, 15, 17, 22, and 24 dpi.; (iii) AGI-5198 has been shown to significantly decrease intratumoral 2HG in-vivo and impair tumor growth in an anaplastic oligodendroglioma patient derived xenograft model when administered daily for 3 weeks with no signs of toxicity (8). Glioma bearing mice were intraperitonially injected with AGI-5198 (40 mg/kg) or saline at 7, 9, 11, 14, 16, 18, 21, 23, 25 dpi. This treatment scheduled significantly decreased intratumoral 2HG (Figure 2B), thus we decided to use this treatment schedule for all *in vivo* studies; (iii) The αPD-L1 antibody was administered to coincide with the peak of AGI-5198+SOC-induced T cell infiltration into the tumor microenvironment to ensure optimal cytotoxic T cell activity. We had previously shown that administration of αPD-L1 to glioma bearing mice treated with immunotherapy at a time point when there is maximal infiltration of tumor antigen-specific T cells in the TME, significantly improved the therapeutic response (9). Glioma bearing mice were injected i.p with

αPD-L1 (8 mg/kg) at 9 and 16 dpi. For survival studies, mice that displayed signs of tumor burden were perfused with Tyrode's solution and paraformaldehyde (PFA). For phenotypic characterization of immune cellular infiltrates, mice were processed for flow cytometry analysis at 27 dpi. For immunological memory response assessment, long-term survivors were rechallenged with mIDH1 glioma cells in the contralateral hemisphere at 90 dpi and processed for flow cytometry analysis at 104 dpi; or the experiment was terminated 60 dpi post tumor rechallenge.

Immunohistochemistry

For immunofluorescence assessment, brain fixed in PFA were serially sectioned 50 µm thick using the vibratome system (Leica VT100S). Sections were placed consecutively into six wells (12-well plate) containing 2 mL of PBS with 0.01% sodium azide. Each well containing sections was a representation the whole brain. For neuropathology assessment, brains fixed in PFA were embedded in paraffin and sectioned 5 µm thick using a microtome system (Leica RM2165. Immunohistochemistry was performed on brain sections by permeabilizing them with TBS-0.5% Triton-X (TBS-TX) for 20 min. This was followed by antigen retrieval at 96 °C with 10 mM sodium citrate (pH 6) for an additional 20 min. Once the sections cooled down to room temperature (RT), they were washed five times (3min per wash) with TBS-TX and blocked with 10% horse serum in TBS-TX for 1 hour at RT. Brain sections were incubated in primary antibody Ki-67 (1:1000), cleaved caspase 3 (1:400), PD-L1 (1:50), GFAP (1:1000), MBP (1:500), or CD8 (1:2000) diluted in 1% horse serum TBS-TX overnight at RT. The next day sections were washed with TBS-TX 5 times. Secondary antibodies were diluted 1:1000 in 1% goat serum TBS-TX. Brain sections labeled with Ki67, CC3, PD-L1, CD8 were incubated in fluorescent-dye conjugated

secondary antibody, while brain sections labeled with GFAP or MBP were incubated with HRP secondary antibody for 4 hours. Brain sections stained with Ki67, CC3, PD-L1, or CD8 were washed in PBS 3 times before being mounted onto microscope slides and cover-slipped with ProLong Gold. High magnification images at 63X were obtained using confocal microscopy (Carl Zeiss: MIC-System) and stains were quantified using ImageJ software. Brain sections stained with MBP and GFAP were incubated with 3, 3′-diaminobenzidine (DAB) (Biocare Medical). The reaction was quenched with 10% sodium azide; sections were washed three times in 0.1 M sodium acetate followed by dehydration in xylene. Once the slides were coverslipped with DePeX Mounting Medium (Electron Microscopy Sciences), they were imaged using brightfield setting at 20X magnification (Olympus BX53).

To quantify tumor size per mouse, vibratome brain sections from a single well were stained with Cresyl Violet as described previously (4, 10, 11). Approximately 5-7 tumor sections per mouse were imaged using the brightfield (Olympus BX53) setting. Area of the Nissl stain covering the tumor couture in the brightfield micrographs was quantified under the Otsu threshold using ImageJ analytical software.

Paraffin embedded 5 μm liver and brain sections were stained with H&E as described by us previously (10). Brightfield images were obtained using Olympus MA BX53 microscope.

Complete Blood Cell Counts and Serum Biochemistry

Blood from mice was taken from the submandibular vein and transferred to EDTA coated microtainer tubes (BD Biosciences) or serum separation tubes (Biotang). For serum collection samples were left in the tubes for 20 min at room temperature to allow for blood coagulation before centrifugation at 2,000 rpm. Complete blood cell counts and serum chemistry for each sample were

determined by in vivo animal core at the University of Michigan. Levels of IL-2 and IL-15 in the serum was measured by ELISA according to manufacturer's instructions (R&D) at the Cancer Center Immunology Core, University of Michigan.

T cell Proliferation Assay

Splenocytes from the spleens of OT-1 knockout mice (Jackson) were labeled with 5-(and 6)-carboxyfluorescein diacetate succinimidyl ester (CFSE) according the manufacturer's instructions (ThermoFisher Scientific). Splenocytes (5.0×10^5) were stimulated with 100nM SIINFEKL peptide (Anaspec) in the presence or absence of 0.25mM, 0.5mM, 5mM, 15mM, and 30mM D-2HG Salt (Sigma-Aldrich) for 4 days in RPMI 1640 media supplemented with 100units/mL Penicilin-Streptomycin and 10% fetal bovine serum. T cells were stained with anti-mouse CD3 and CD8 antibodies, and proliferation was assessed by CFSE dye dilution using a flow cytometer. Levels of IFN-γ in the cultures' supernatants was measured by ELISA according to manufacturer's instructions (R&D) at the Cancer Center Immunology Core, University of Michigan. T cell apoptosis induced by D-2HG was identified by staining cells with Annexin V-FITC (ThermoFisher) in 1X Annexin V binding buffer and 1ug/mL propidium iodide (PI). CD8+/CD3+ T cells with positive staining for both Annexin V and PI staining were identified as dead cells. CD8+/CD3+ T cells with negative staining for both Annexin V and PI staining were identified as live cells.

Flow cytometry

Mice were euthanized and tumors were dissected from the brain and made into single cell suspensions. Blood was subjected to Red Blood Cell lysis at room temperature for 10 minutes.

Tumor infiltrating immune cells in the brain was enriched with 30%70% Percoll (GE Lifesciences) density gradient. These cells were resuspended in flow buffer and non-specific antibody binding was blocked with anti-CD16/CD32. Dendritic cells were labeled with CD45, CD11c, CD80, CD86, MHC II and B220 antibodies. M1 macrophages were labeled with CD45 and F4/80 antibodies. M2 macrophages were labeled with CD45, F4/80 and CD206 antibodies. Tumor specific T cells were labeled with CD45, CD3, CD8 and SIINFEKL-H2Kb-tetramer. Memory T cells were labeled with CD45, CD3, CD8, CD44, and CD62L antibodies. Exhausted T cells were labeled with CD45, CD3, CD8, PD-1, TIM-3, and TIGIT antibodies. MDSCs were labeled with CD45, Gr-1, or Ly6G and CD11b antibodies. Tregs were labeled with CD45, CD4, CD25, and Foxp3, using the Foxp3 staining kit from BD. Intracellular IFNγ were stained using BD intracellular staining kit using the manufacturer's instructions. Antibody staining was carried out for 30 min at 4°C. Staining was performed in the following order with three washes between each step: live/dead staining, Fc blocking, surface staining, cell fixation, intracellular staining and data acquisition. Flow data has been measured BD FACS ARIA SORP (BD Bioscience) and analyzed (Supplementary Figure 25) using Flow Jo version 10 (Treestar).

TCGA analysis

TCGA gene expression data was analyzed using the GlioVis data visualization tool, which contains over 6500 tumor samples of approximately 50 expression datasets of a large collection of brain tumor entities (12). That includes TCGA data for WHO grade II, III and IV glioma patients. Data on IDH1 mutation status was obtained for each patient using http://gliovis. bioinfo.cnio.es portal. Cases were stratified into 2 groups on the basis of wild type (288 cases) or mutated (655 cases) IDH status. Based on genetic lesions within the tumors, they were either classified as IDH1

mutant codel (1p/19q intact), IDH1 mutant noncodel (TP53/ATRX loss), or WtIDH. Log2 gene expression levels of CD274 (PD-L1) within WtIDH and mIDH1 patients was compared using Tukey's Honest Significant Difference (HSD) statistical test. For the TCGA DNA methylation analysis of WtIDH and mIDH1 glioma patients, five probes with enriched methylation (Cg15837913, Cg19724470, Cg14305799, Cg13474877, and Cg02823866) within the CpG island were chosen to determine DNA methylation levels for CD274 based on previously described findings by *Mu et al* (13). TCGA CD274 DNA methylation analysis was also carried out for WtIDH and mIDH1 acute myeloid leukemia (AML) patients. The β-values for DNA methylation levels at the CpG sites were determined using Mexpress (14). The β-values were determined as the ratio between methylated probe signal relative to the total (methylated and unmethylated) probe signal. The β-value, ranging from 0.00 to 1.00 represents enriched methylation level of the individual CpG probe.

Western Blot

Mouse mIDH1 neurospheres and human mIDH1 neurospheres (SJGBM2-mIDH1) were seeded at density of 1.0 x 10^6 cells into 25-cm^2 flasks containing NSC media. After 24 hours, mouse neurospheres and human glioma cells were treated with 5Gy and 10Gy radiation respectively. After an additional 48 hours, cell lysates were prepared by incubating glioma cells with protease inhibitors and 0.5 mL RIPA lysis buffer on ice for 5 minutes. Resulting cell lysates were centrifuged at 13000 RPM at 4°C for 10 minutes and supernatants were collected to determine protein concertation in comparison to standard bovine serum albumin (BSA) protein concentrations through bicinchoninic acid assay (BCA). For electrophoretic separation of proteins, twenty-five micrograms of total protein were resuspended in loading buffer (10% sodium dodecyl sulfate, 20% glycerol, and 0.1% bromophenol blue) and incubated for 5 minutes at 95°C for 10 minutes to be loaded onto a 4-12% Bis-Tris gel. Proteins from the gel were transferred to 0.2 µm

nitrocellulose membrane and blocked with 5% nonfat milk in TBS-0.1% Tween-20. After blocking, membranes were incubated with primary anti-LCI/II (1:1000), Vinculin (1:1000), or β-Actin (1:1000) overnight at 4°C. The next day, blots were washed with TBS-0.1% tween-20 and incubated with secondary (1:4000) antibody for one hour at room temperature. Blots were washed several times again with TBS-0.1% tween-20 and visualized under Biorad gel imaging software. Band intensities were quantified using ImageJ software.

PD-L1 and MGMT Methylation Levels

Mouse and human (SF10602) glioma cells were seeded at density of 1.0 x 10^6 cells into 25-cm^2 flasks containing media. Mouse cells were treated with 1.5 μM AGI-5198; human glioma cells were treated with 5μM AGI-5198. DMSO was utilized as vehicle control. Cells were maintained in culture for ten days, media containing AGI-5198 or vehicle control was replaced every 2 days. On day ten, genomic DNA was extracted from cells in the 25-cm^2 flasks using Qiagen DNA extraction kit according to manufactures instructions. To identify amplification targets on PD-L1 and MGMT promoters, CpG elements were located in the region downstream of the transcription start site (TTS) of each gene using MethPrimer (15). For mouse PD-L1 gene, a CpG island was found between -57 and -197 bp with respect to the TTS (Supplementary Figure 26). For mouse MGMT promoter, a region containing CpG was identified between -50 and -250 bp with respect to the TTS (Supplementary Figure 24). For the human PD-L1 gene, we used primers previously described to analyze promoter methylation (16). PD-L1 or MGMT methylation levels within the cells were determined using OneStep qMethyl-Lite kit (Zymo Research). Briefly, for each qPCR reaction, 20 ng of DNA were incubated in the presence (Test sample) or absence (Reference sample) of methyl-sensitive restriction enzymes at 37°C for 2 hours (Supplemental Figure 9). After the methylation-sensitive restriction enzymes reaction (MSRE), the test and reference samples

were respectively mixed with Fast SYBR® Green Master Mix to a concentration 1X and with forward and reverse primers at a concentration of 0.5 μM each. Quantitative PCR (qPCR) were run using the ViiA 7 Real-Time PCR System (Life Technolgies). The PCR program included initial denaturation at 95°C for 10 min followed by 45 cycles of 95°C for 15s and 60°C for 60s. Percentage methylation was determined using the formula $100 \times 2^{-\Delta Ct}$, where ΔCt is the difference of Ct value between the reference and test samples. The primers used are listed in Table 10.

Sex Determination of Mouse Glioma Neurospheres

Genomic DNA was extracted from 1.0 x 10^6 WtIDH and mIDH1 mouse neurospheres using DNeasy Blood & Tissue Kit (Quiagen™) extraction kit according to manufactures instructions. Neurosphere lysates were heated to 95 °C for 15 min, cooled to room temperature. Genomic DNA extracted from blood of a male and a female C57BL6 mouse, respectively were used as positive control for both genders. 1 μl of gDNA at a concentration of 200 ng/μl was combined with 19 μl PCR reaction master mix containing 1X buffer (1:2 of DreamTaq Green PCR Master Mix (2X), Thermo Scientific™ Cat # K1081), 10 μM forward primer (CACCTTAAGAACAAGCCAATACA), 10 μM reverse primer (GGCTTGTCCTGAAAACATTTGG) (17). Thermocycler conditions were set to the following parameters: 94 °C for 2 min, followed by 30 cycles of 94 °C for 20 s, 60 °C for 20 s and 72 °C for 30 s, and a final elongation step at 72 °C for 5 min. PCR reactions were loaded on to a 1% agarose gel containing 1:l0000 of SYBR Safe DNA Gel Stain (17). The gel was run at 90V for 30 min in 1X TAE buffer (40 mM Tris acetate, 2 mM Na_2EDTA) and visualized using the Biorad gel imaging software.

Statistical analysis

Sample sizes were selected based on preliminary data from pilot experiments and published results in the literature and our laboratory. Animal studies were performed after randomization. Unpaired Student t-test or one-way analysis of variance (ANOVA), followed by Tukey's multiple comparisons post-test were utilized for comparing experimental groups with controls from immunofluorescence, tumor size quantification, flow cytometry analysis and T cell functional assays. Turkey's Honest Significant Difference test was utilized to comparing glioma patient groups from TCGA. Kaplan-Meier methods were used to construct survival functions and estimate the median survival, and Log-rank (Mantel-Cox) were used to compare the survival functions between treatment groups. P-values were adjusted using the Tukey–Kramer method (18). The 90-day survival rates were estimated using the Kaplan-Meier method, and the hazard ratios (HRs) were estimated using the Cox proportional hazard model (18). Data were analyzed using Prism 6.0 (GraphPad Software). Data were normally distributed so that the variance between groups was similar. P values less than 0.05 were considered statistically significant. Values are reported as means ± SD with the indicated sample size. No samples were excluded from analysis.

References

1. Kang MH, Smith MA, Morton CL, Keshelava N, Houghton PJ, and Reynolds CP. National Cancer Institute pediatric preclinical testing program: model description for in vitro cytotoxicity testing. *Pediatric blood & cancer.* 2011;56(2):239-49.
2. Tateishi K, Wakimoto H, Iafrate AJ, Tanaka S, Loebel F, Lelic N, Wiederschain D, Bedel O, Deng G, Zhang B, et al. Extreme Vulnerability of IDH1 Mutant Cancers to NAD+ Depletion. *Cancer Cell.* 2015;28(6):773-84.
3. Jones LE, Hilz S, Grimmer MR, Mazor T, Najac C, Mukherjee J, McKinney A, Chow T, Pieper RO, Ronen SM, et al. Patient-derived cells from recurrent tumors that model the evolution of IDH-mutant glioma. *Neuro-oncology advances.* 2020;2(1):vdaa088.
4. Nunez FJ, Mendez FM, Kadiyala P, Alghamri MS, Savelieff MG, Garcia-Fabiani MB, Haase S, Koschmann C, Calinescu AA, Kamran N, et al. IDH1-R132H acts as a tumor suppressor in glioma via epigenetic up-regulation of the DNA damage response. *Science translational medicine.* 2019;11(479).
5. Leder K, Pitter K, LaPlant Q, Hambardzumyan D, Ross BD, Chan TA, Holland EC, and Michor F. Mathematical modeling of PDGF-driven glioblastoma reveals optimized radiation dosing schedules. *Cell.* 2014;156(3):603-16.
6. Halliday J, Helmy K, Pattwell SS, Pitter KL, LaPlant Q, Ozawa T, and Holland EC. In vivo radiation response of proneural glioma characterized by protective p53 transcriptional program and proneural-mesenchymal shift. *Proceedings of the National Academy of Sciences of the United States of America.* 2014;111(14):5248-53.
7. Mathieu V, De Nève N, Le Mercier M, Dewelle J, Gaussin JF, Dehoux M, Kiss R, and Lefranc F. Combining bevacizumab with temozolomide increases the antitumor efficacy of temozolomide in a human glioblastoma orthotopic xenograft model. *Neoplasia (New York, NY).* 2008;10(12):1383-92.
8. Rohle D, Popovici-Muller J, Palaskas N, Turcan S, Grommes C, Campos C, Tsoi J, Clark O, Oldrini B, Komisopoulou E, et al. An inhibitor of mutant IDH1 delays growth and promotes differentiation of glioma cells. *Science (New York, NY).* 2013;340(6132):626-30.
9. Kamran N, Kadiyala P, Saxena M, Candolfi M, Li Y, Moreno-Ayala MA, Raja N, Shah D, Lowenstein PR, and Castro MG. Immunosuppressive Myeloid Cells' Blockade in the Glioma Microenvironment Enhances the Efficacy of Immune-Stimulatory Gene Therapy. *Molecular therapy : the journal of the American Society of Gene Therapy.* 2017;25(1):232-48.
10. Calinescu AA, Yadav VN, Carballo E, Kadiyala P, Tran D, Zamler DB, Doherty R, Srikanth M, Lowenstein PR, and Castro MG. Survival and Proliferation of Neural Progenitor-Derived Glioblastomas Under Hypoxic Stress is Controlled by a CXCL12/CXCR4 Autocrine-Positive Feedback Mechanism. *Clin Cancer Res.* 2017;23(5):1250-62.
11. Kadiyala P, Li D, Nunez FM, Altshuler D, Doherty R, Kuai R, Yu M, Kamran N, Edwards M, Moon JJ, et al. High-Density Lipoprotein-Mimicking Nanodiscs for Chemo-immunotherapy against Glioblastoma Multiforme. *ACS nano.* 2019;13(2):1365-84.

12. Bowman RL, Wang Q, Carro A, Verhaak RG, and Squatrito M. GlioVis data portal for visualization and analysis of brain tumor expression datasets. *Neuro-oncology.* 2017;19(1):139-41.
13. Mu L, Long Y, Yang C, Jin L, Tao H, Ge H, Chang YE, Karachi A, Kubilis PS, De Leon G, et al. The IDH1 Mutation-Induced Oncometabolite, 2-Hydroxyglutarate, May Affect DNA Methylation and Expression of PD-L1 in Gliomas. *Front Mol Neurosci.* 2018;11(82.
14. Wei J, Li G, Zhang J, Zhou Y, Dang S, Chen H, Wu Q, and Liu M. Integrated analysis of genome-wide DNA methylation and gene expression profiles identifies potential novel biomarkers of rectal cancer. *Oncotarget.* 2016;7(38):62547-58.
15. Li L-C, and Dahiya R. Methprimer: Designing Primers for Methylation PCRs. *Bioinformatics (Oxford, England).* 2002;18:427-31.
16. Asgarova A, Asgarov K, Godet Y, Peixoto P, Nadaradjane A, Boyer-Guittaut M, Galaine J, Guenat D, Mougey V, Perrard J, et al. PD-L1 expression is regulated by both DNA methylation and NF-kB during EMT signaling in non-small cell lung carcinoma. *Oncoimmunology.* 2018;7(5):e1423170.
17. Tunster SJ. Genetic sex determination of mice by simplex PCR. *Biol Sex Differ*. 2017; 8(31): 1-4.
18. Cox DR. Regression models and life-tables. *Journal of the Royal Statistical Society: Series B (Methodological)*. 1972 Jan;34(2):187-202.

Supplementary Figure 1

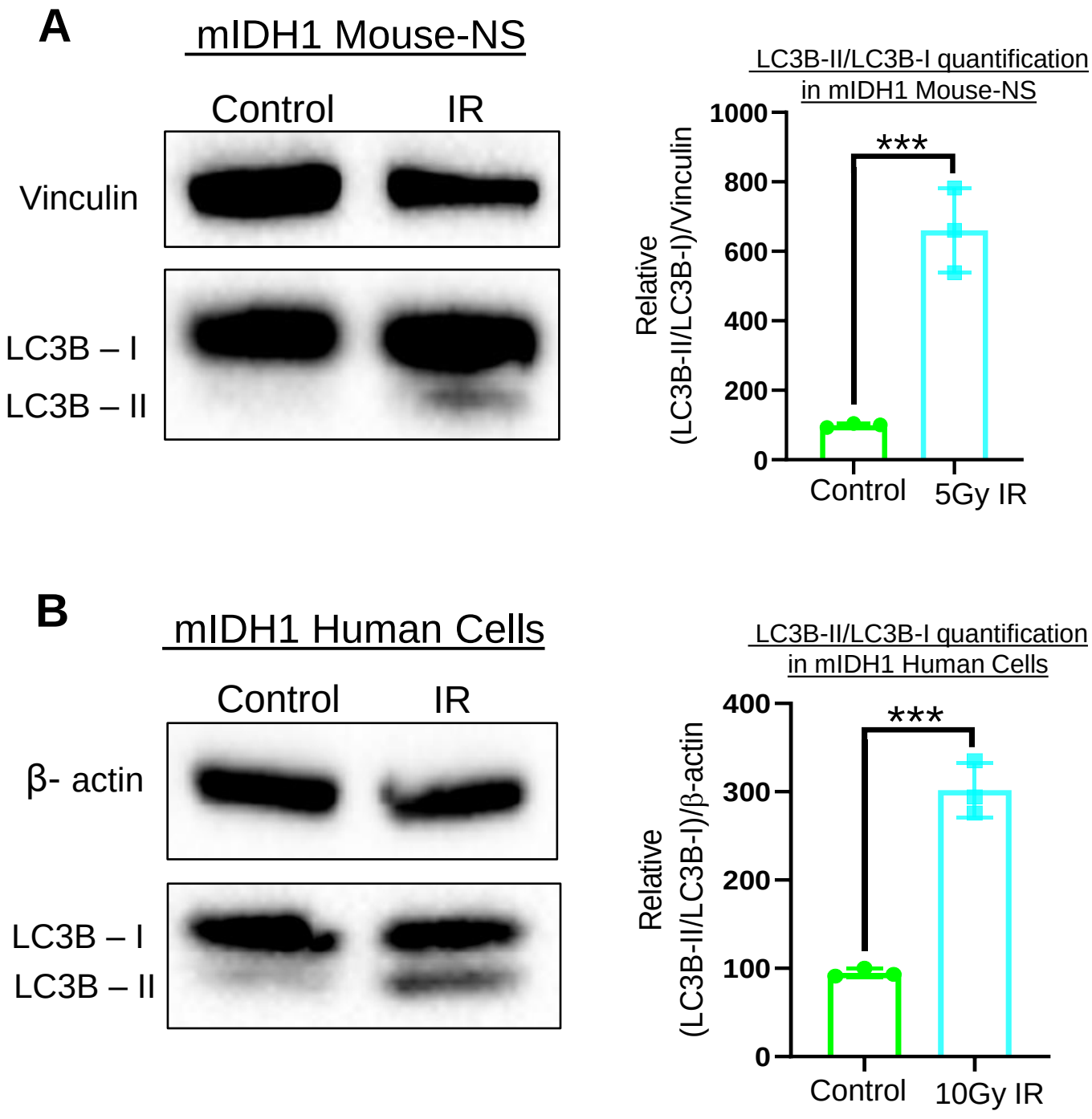

Supplementary Figure 1: Radiotherapy promotes activation of autophagy in mIDH1 mouse-NS and human-GC. (**A**) Mouse-NS were treated with 5 Gy IR for 48 hrs. Western blot analysis of LC3B expression. Vinculin: loading control. Bar graph represents semi-quantification of (LC3B-II/LC3B-I)/vinculin. (**B**) Human-GC (SGJBM2-mIDH1) were treated with 10 Gy IR for 48 hrs. Western blot analysis of LC3B expression. β-actin: loading control. Bar graph represents semi-quantification of (LC3B-II/LC3B-I)/β-actin. *** $P < 0.001$; one-way ANOVA. Data shown as ± SEM ($n = 3$ technical replicates).

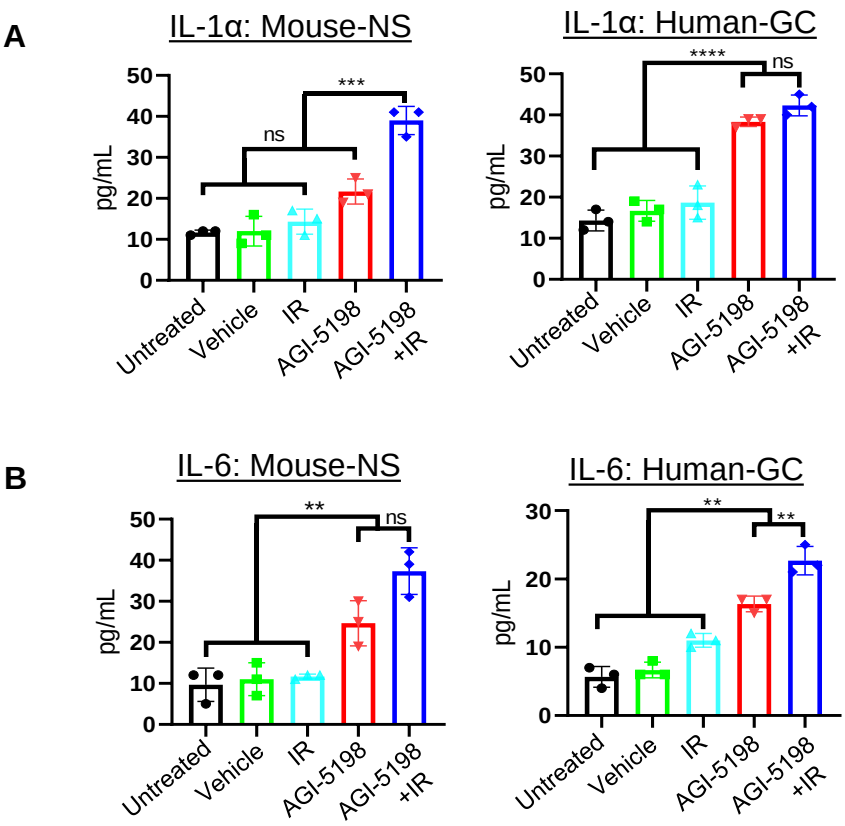

Supplementary Figure 2: Inhibition of IDH1-R132H in combination with radiotherapy promotes the release of IL1-1α and IL-6 by mIDH1 mouse-NS and human-GC. (**A, B**) Mouse-NS were treated with 3 Gy IR in combination 1.5 μM of AGI-5198 for 72 hrs. Human-GC were treated with 10 Gy IR in combination with 5μM of AGI-5198 for 72 hrs. (A) Quantification of IL-1α release in the supernatant of mIDH1 Mouse-NS and Human-GC. (B) Quantification of IL-6 release in the supernatant of mIDH1 Mouse-NS and Human-GC. ***P* < 0.01, ****P* < 0.001, *****P* < 0.0001, one-way ANOVA test. Bars represent mean ± SEM (*n* = 3 technical replicates).

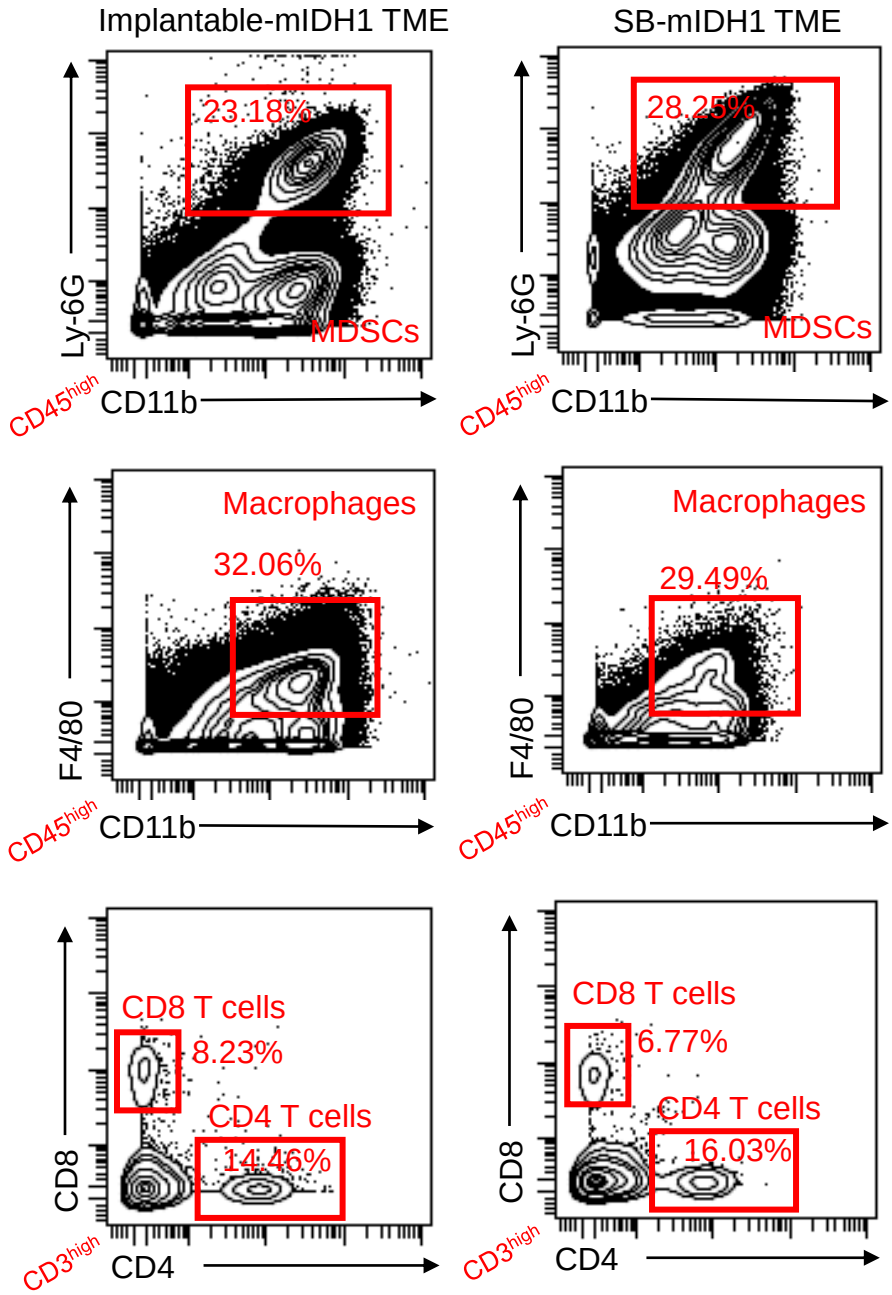

Supplementary Figure 3: Frequency of tumor-infiltrating immune cells in the TME of sleeping beauty (SB) and implanted mIDH1 glioma bearing mice. Quantification of the percent of MDSCs ($CD11b^+/Ly6G^+$), Macrophages ($CD11b^+/F4/80^+$), CD8 T cells ($CD3^+/CD8^+$) and CD4 T cells ($CD3^+/CD4^+$) within the $CD45^+$ cell population in the TME of SB or implanted mIDH1 glioma bearing mice. Immune cellular infiltrates in the TME were assessed when animals displayed signs of tumor burden. Representative flow plots for each group are displayed (*n* = 3 biological replicates).

Chromatograms for *in vivo* D-HG Quantification

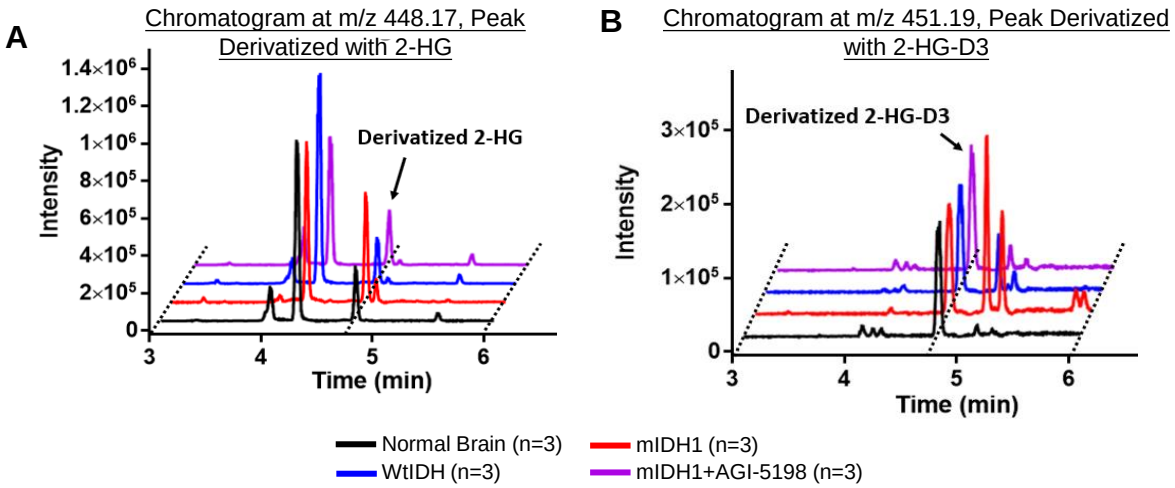

Supplementary Figure 4: Inhibition of IDH1-R132H decreases the production of 2HG *in vivo*. UPLC-MS analysis to assess the D-2HG concentration in the TME of normal mice (blank; black), WtIDH glioma bearing mice (blue), mIDH1 glioma bearing mice (red), and mIDH1 glioma bearing mice treated with AGI-5198 (purple). Chromatogram to the left was acquired at m/z 448.17 (-), peak at 4.8 min is derivatized 2-HG. Chromatogram to the right was acquired at m/z 451.19 (-), peak at 4.8 min is derivatized 2-HG-D3.

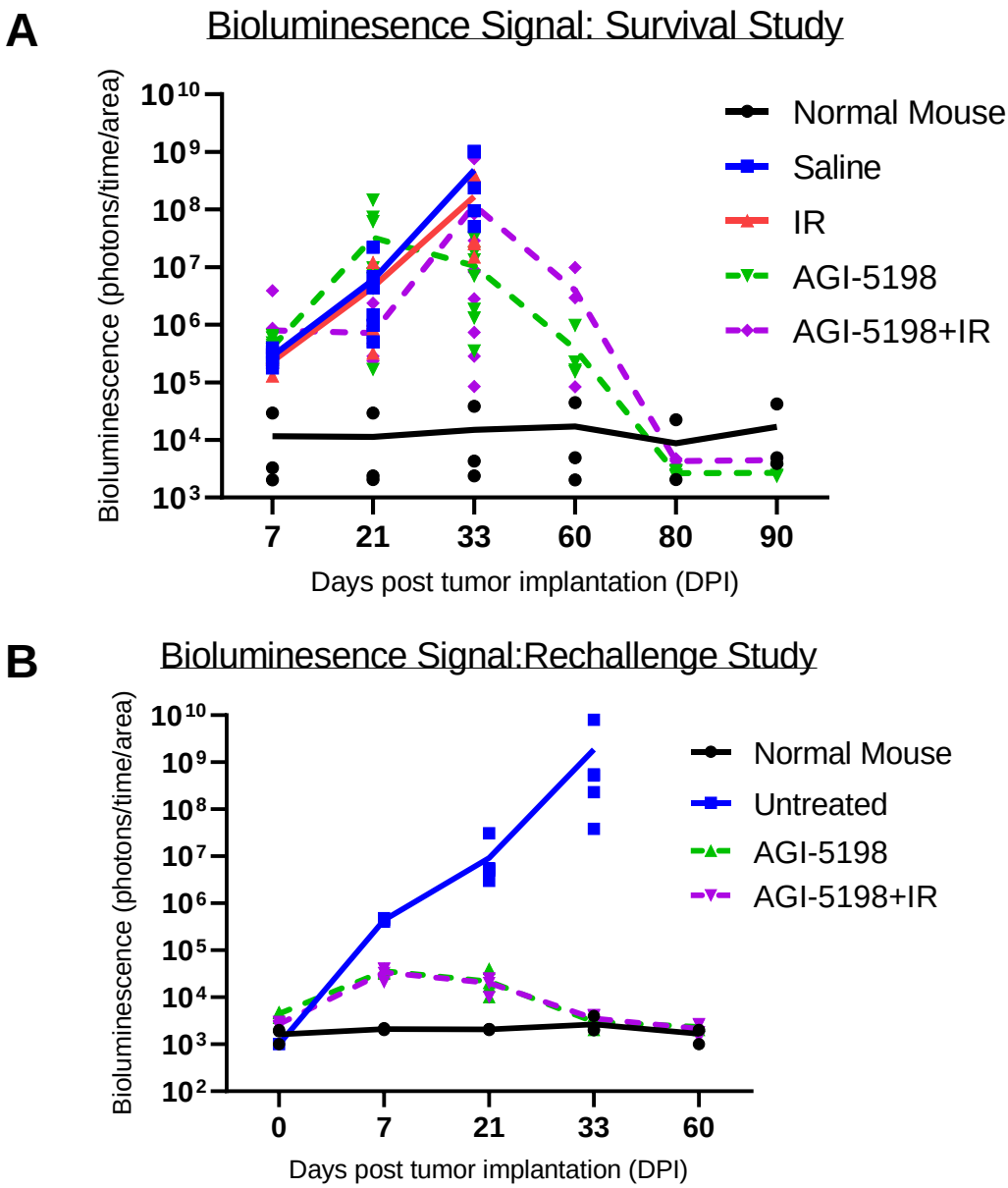

Supplementary Figure 5: Mutant IDH1 glioma growth *in vivo* in response to IDH1-R123H inhibition alone or in combination with radiation. **(A)** Bioluminescence monitoring of mIDH1 glioma growth in mice after treatment with saline (*n* = 7 biological replicates), IR (*n* = 6 biological replicates), AGI-5198 (*n* =10 biological replicates), or AGI-5198+IR (*n* = 10 biological replicates). Tumor growth was monitored at sequential time points during the survival study. **(B)** Bioluminescence monitoring of mIDH1 glioma growth in rechallenged long-term survivors from AGI-5198 (*n* = 4 biological replicates), AGI-5198+IR (*n* = 4 biological replicates), or untreated animals (n = 6 biological replicates). Tumor growth was monitored at sequential time points post-tumor implantation in all groups. Bioluminescence signal was also monitored in non-tumor bearing normal mice (n = 3 biological replicates) at sequential time points during the tumor-rechallenge study. The luminescence intensity (photons/time/area) correlates with tumor burden.

Supplementary Figure 6

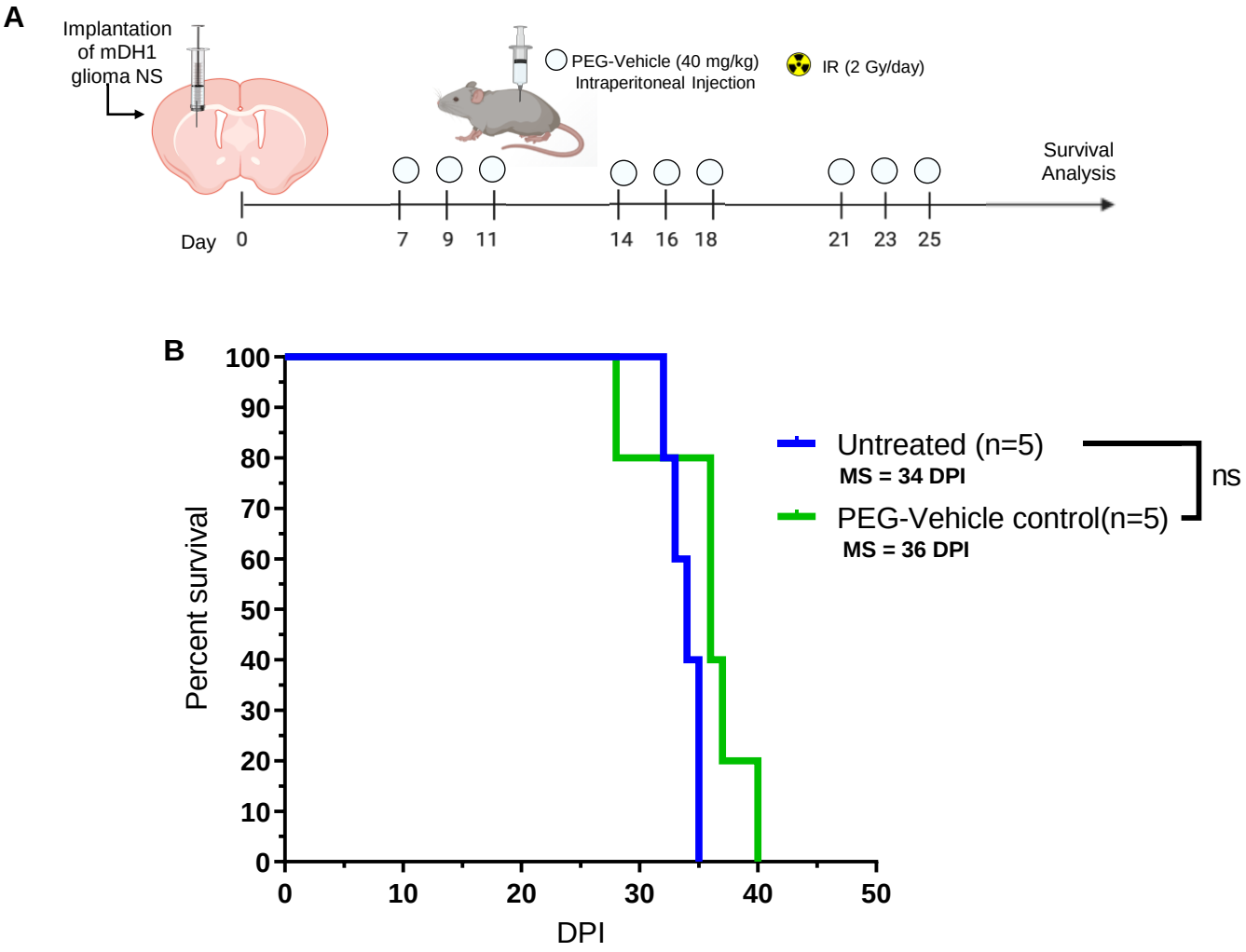

Supplementary Figure 6: Treatment with PEG-vehicle control does not impact the survival of mIDH1 tumor bearing mice. (A) Diagram of the experimental design to assess the effect of PEG-vehicle control on the survival of mIDH1 glioma bearing mice. (**B)** Kaplan-Meier survival analysis of saline (*n* = 5 biological replicates) and vehicle control (*n* = 5 biological replicates). Data were analyzed using the log-rank (Mantel-Cox) test (ns = non-significant; MS = median survival).

Long-Term Survivors after tumor rechallenge (60dpi) stained with Nissl

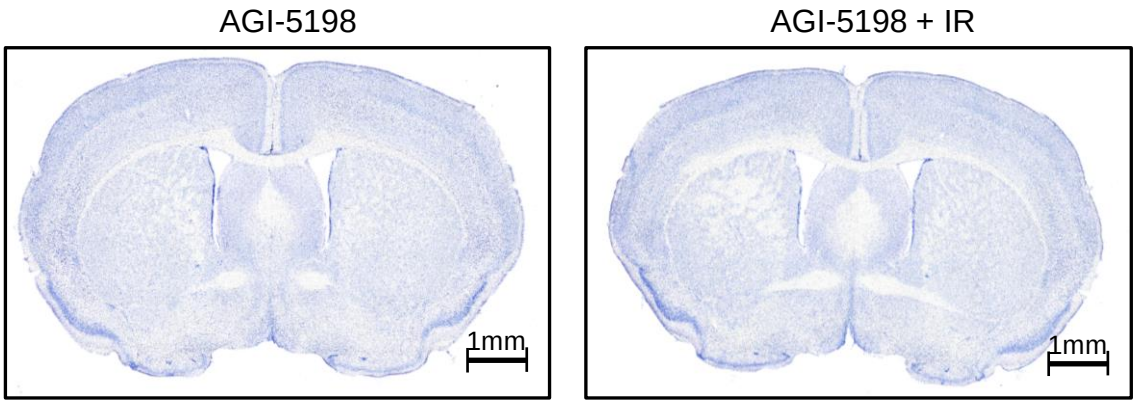

Supplementary Figure 7: Brain sections of tumor rechallenged mice from the IDH1-R123H inhibition and radiotherapy survival study show no evidence of tumor growth. Representative images of 50 µm brain sections of long-term survivors from AGI-5198 or AGI-5198+IR (60 dpi after rechallenge with mIDH1 NS) stained with nissl (*n* = 2 biological replicates).

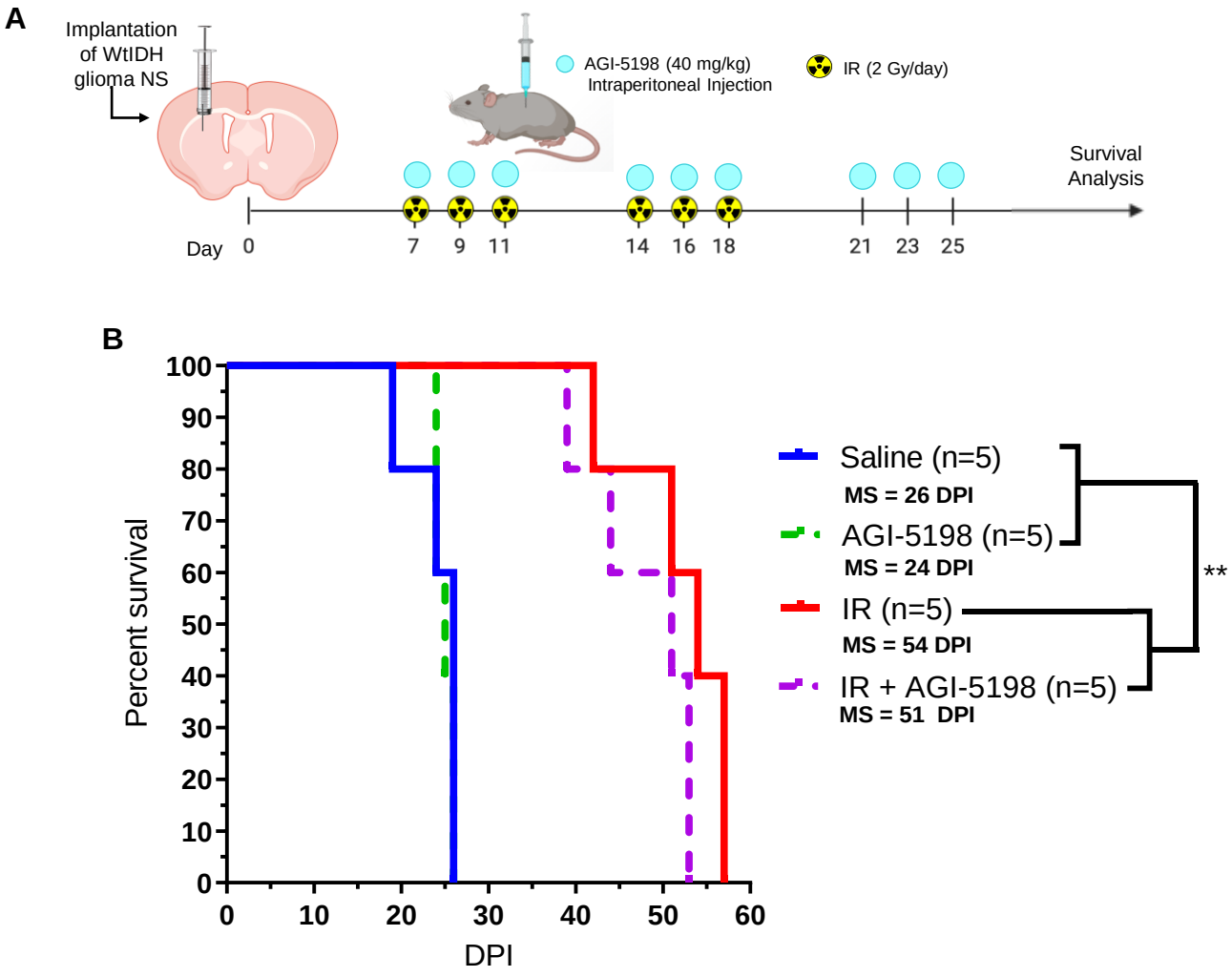

Supplementary Figure 8: Inhibition of IDH1-R132H does not improve the survival of wtIDH1 tumor bearing mice. (A) Diagram of the experimental design to assess the impact of AGI-5198 treatment in combination with radiation on the survival of WtIDH glioma bearing mice. (**B)** Kaplan-Meier survival analysis of saline (*n* = 5 biological replicates, AGI-5198 (*n* = 5 biological replicates), IR (*n* = 5 biological replicates), and IR+AGI-5198 (*n* = 5 biological replicates) treated mice. Data were analyzed using the log-rank (Mantel-Cox) test. ***P* < 0.01; MS = median survival.

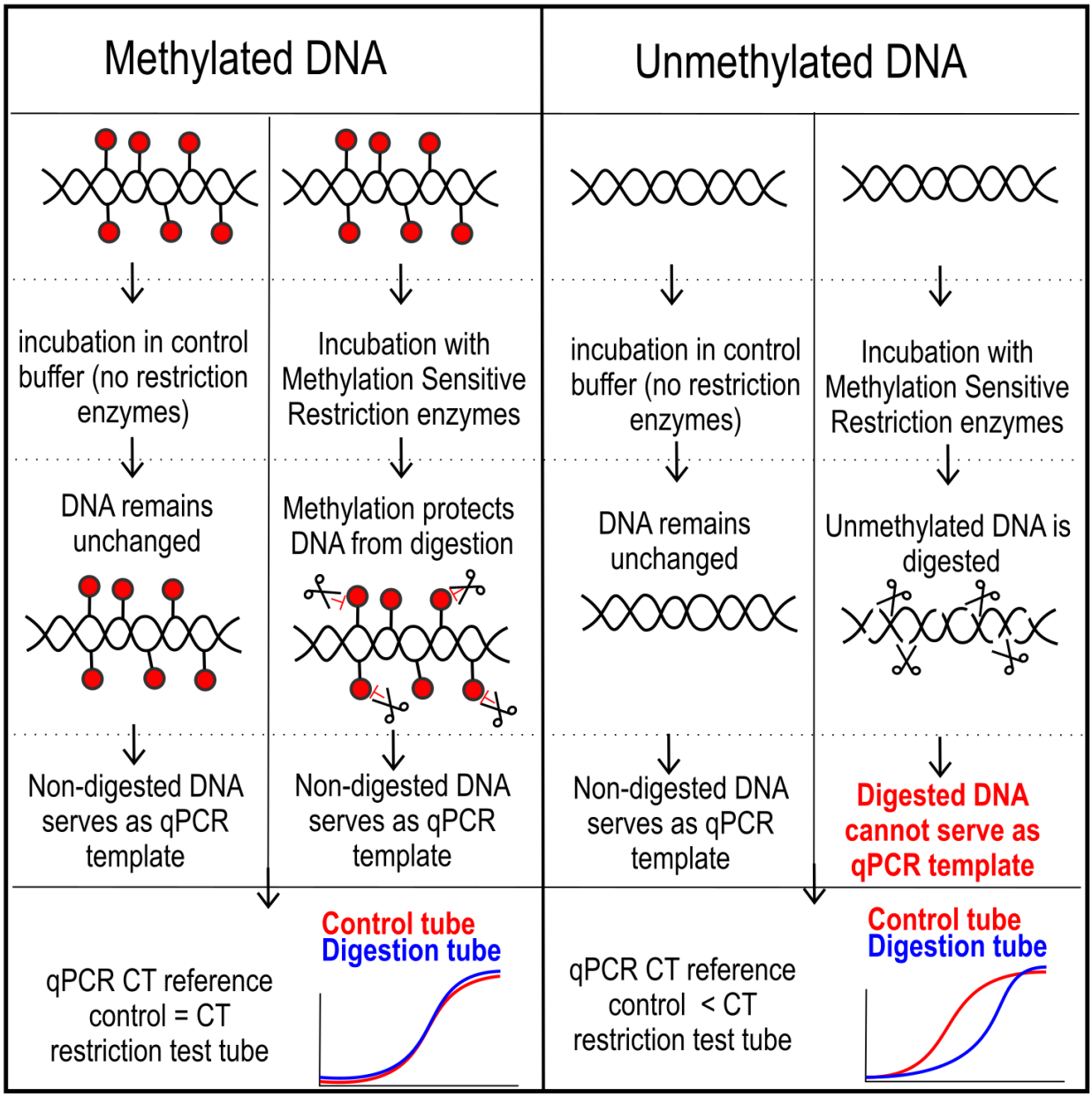

Supplementary Figure 9: Scheme depicting the experimental design applied to determine CD274 (PD-L1) and MGMT DNA methylation status within glioma cells. Genomic DNA (gDNA) extracted from glioma cells was subjected to Methylation-Sensitive Restriction Enzymes (MSREs) digestion. MSREs cannot digest methylated DNA, thus loci where the DNA is methylated are protected from digestion. Quantitative PCR (qPCR) was used to assess the extent of methylated DNA digestion. Digested DNA result in a reduction of the qPCR threshold cycle (CT).

mIDH1 Mouse NS: Vehicle

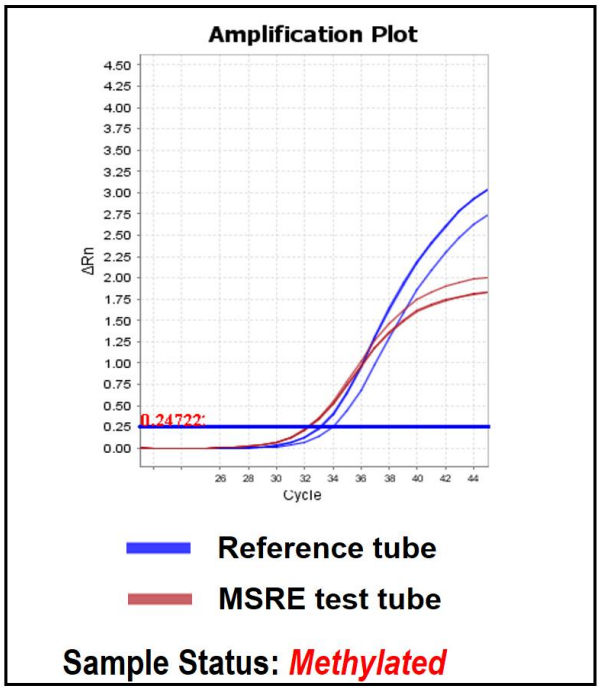

mIDH1 Mouse NS: AGI-5198

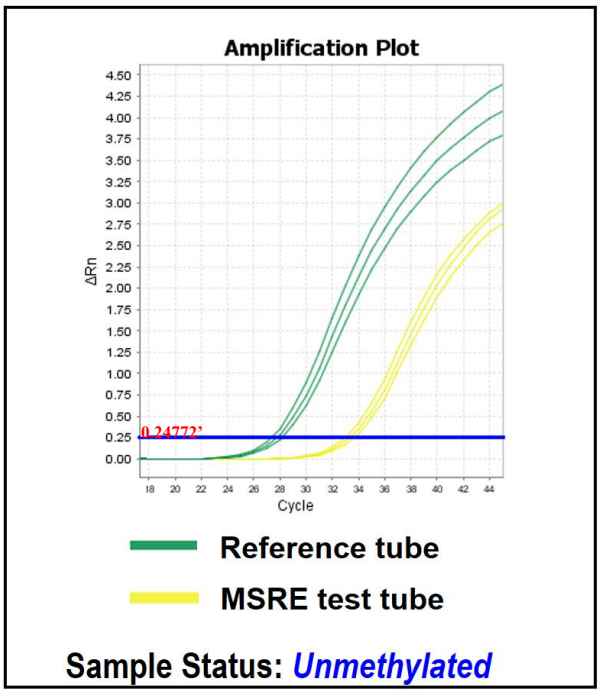

WtIDH Mouse NS: Vehicle Control

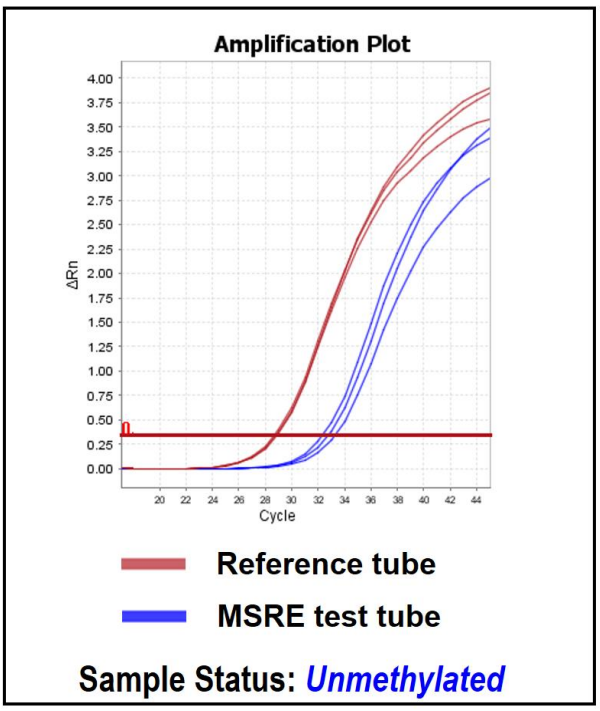

WtIDH Mouse NS: AGI-5198

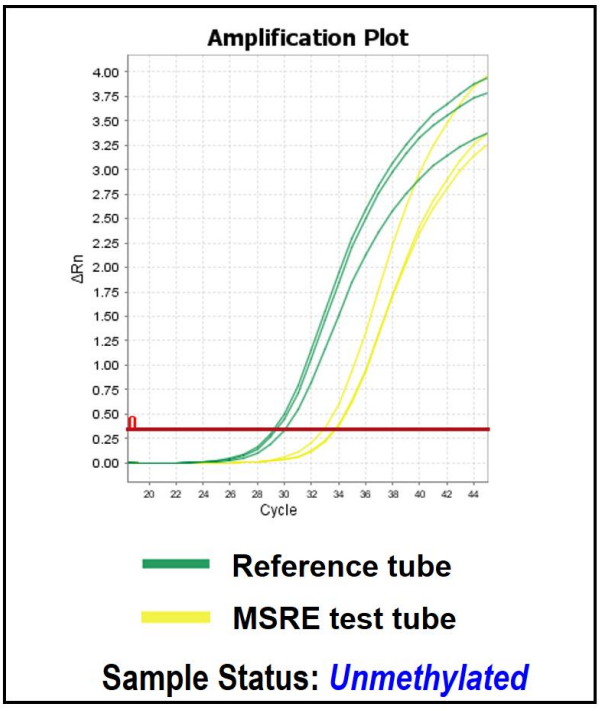

Supplementary Figure 10: Inhibition of IDH1-R132H decreases CD274 (PD-L1) methylation levels in mouse mIDH1 glioma NS. Methylation specific qPCR was performed to assess the PD-L1 promoter methylation status in mIDH1 or WtIDH mouse NS after treatment with 1.5 μM of AGI-5198 or vehicle. Representative qPCR plots from *n* = 3 technical replicates for each treatment condition are displayed. MSRE = Methylation-Sensitive Restriction Enzymes

Supplementary Figure 11

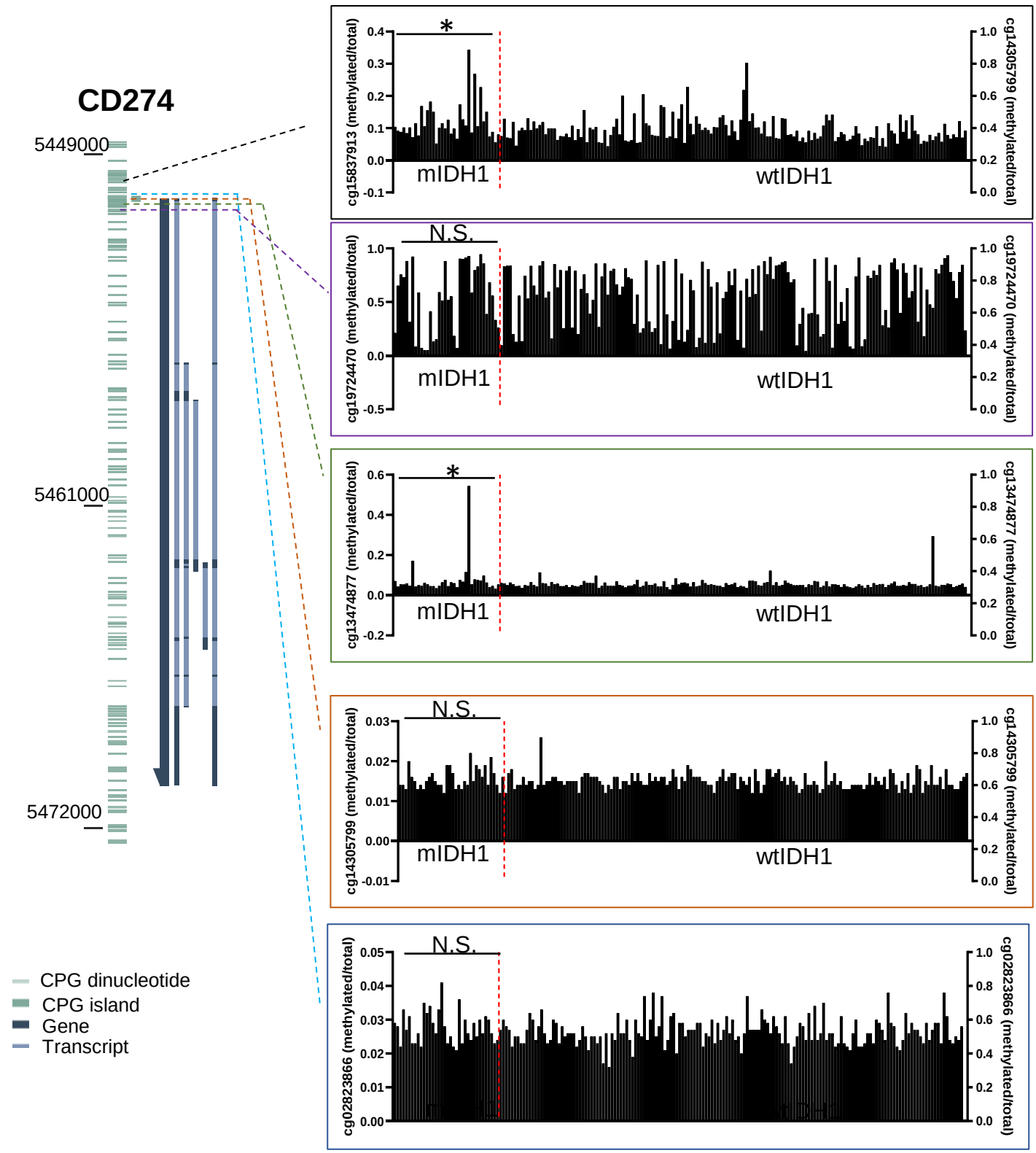

Supplementary Figure 11: IDH1-R132H does not alter CD274 (PD-L1) methylation levels in acute myeloid leukemia (AML) patients. DNA methylation levels within cg15837913, cg19724470, cg14305799, cg13474877, or cg02823866 probes in the CpG island of CD274 promoter were determined for mIDH1 (n = 185) and wtIDH (n = 35) AML patients. Each black bar represents one patient. DNA Methylation status was assessed for TCGA data using Mexpress. *P < 0.05; ns = non-significant, Tukey's Honest Significant Difference test.

mIDH1 human cells: Vehicle Control

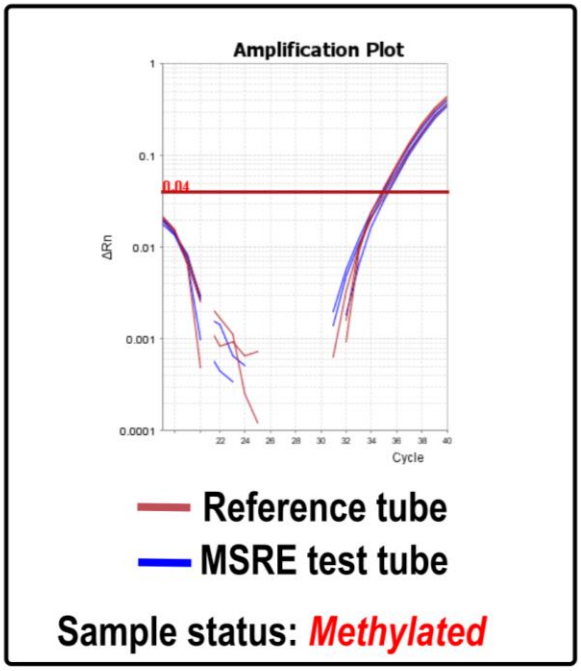

mIDH1 human cells: AGI-5198

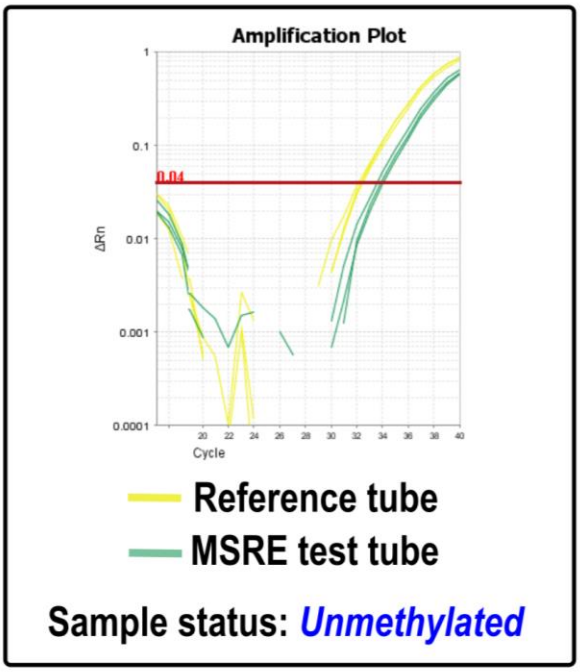

Supplementary Figure 12: Inhibition of IDH1-R132H decreases CD274 (PD-L1) methylation levels in human mIDH1 glioma cells. Methylation specific qPCR was performed to assess the PD-L1 promoter methylation status in mIDH1 human glioma cells after treatment with 5 μM of AGI-5198 or vehicle. Representative qPCR plots from *n* = 3 technical replicates for each treatment condition are displayed. MSRE = Methylation-Sensitive Restriction Enzymes.

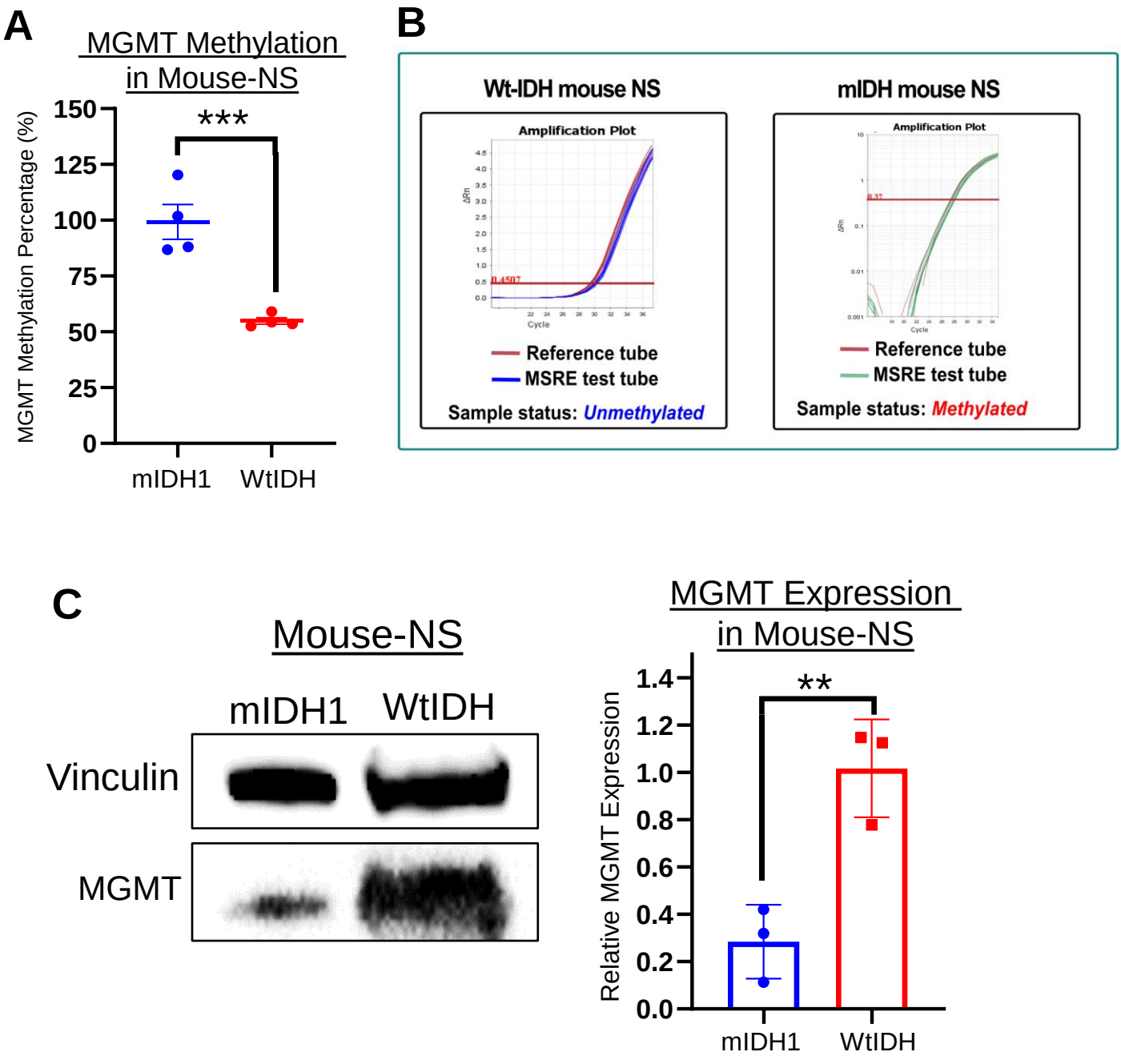

Supplementary Figure 13: IDH1-R132H mouse cells exhibit increased MGMT promoter methylation. (**A**) Quantification of MGMT promoter methylation levels in mIDH1 or WtIDH mouse NS. ***$P < 0.001$; unpaired student t-test. Bars represent mean ± SEM ($n = 3$ technical replicates). (**B**) Representative qPCR plots from $n = 3$ technical replicates for each treatment condition are displayed. MSRE = Methylation-Sensitive Restriction Enzymes. (**C**) Western blot analysis of MGMT expression in mIDH1 or wtIDH mouse NS. Vinculin: loading control. Bar graph represents semi-quantification of relative MGMT expression/Vinculin. ** $P < 0.01$; one-way ANOVA. Data shown as ± SEM ($n = 3$ technical replicates).

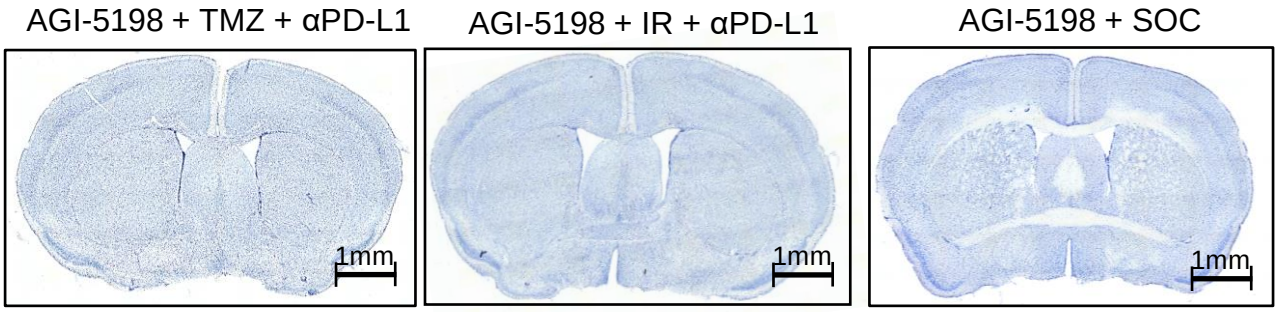

Supplementary Figure 14: Brain sections of tumor rechallenged mice from the IDH1-R123H inhibition, standard of care, and αPD-L1 immune checkpoint blockade survival study show no evidence of tumor growth. Representative images of 50 µm brain sections of long-term survivors from AGI-5198+TMZ+αPD-L1, AGI-5198+IR+αPD-L1, or AGI-5198+SOC (60 dpi after rechallenge with mIDH1 NS) stained with Nissl. (*n* = 2 biological replicates).

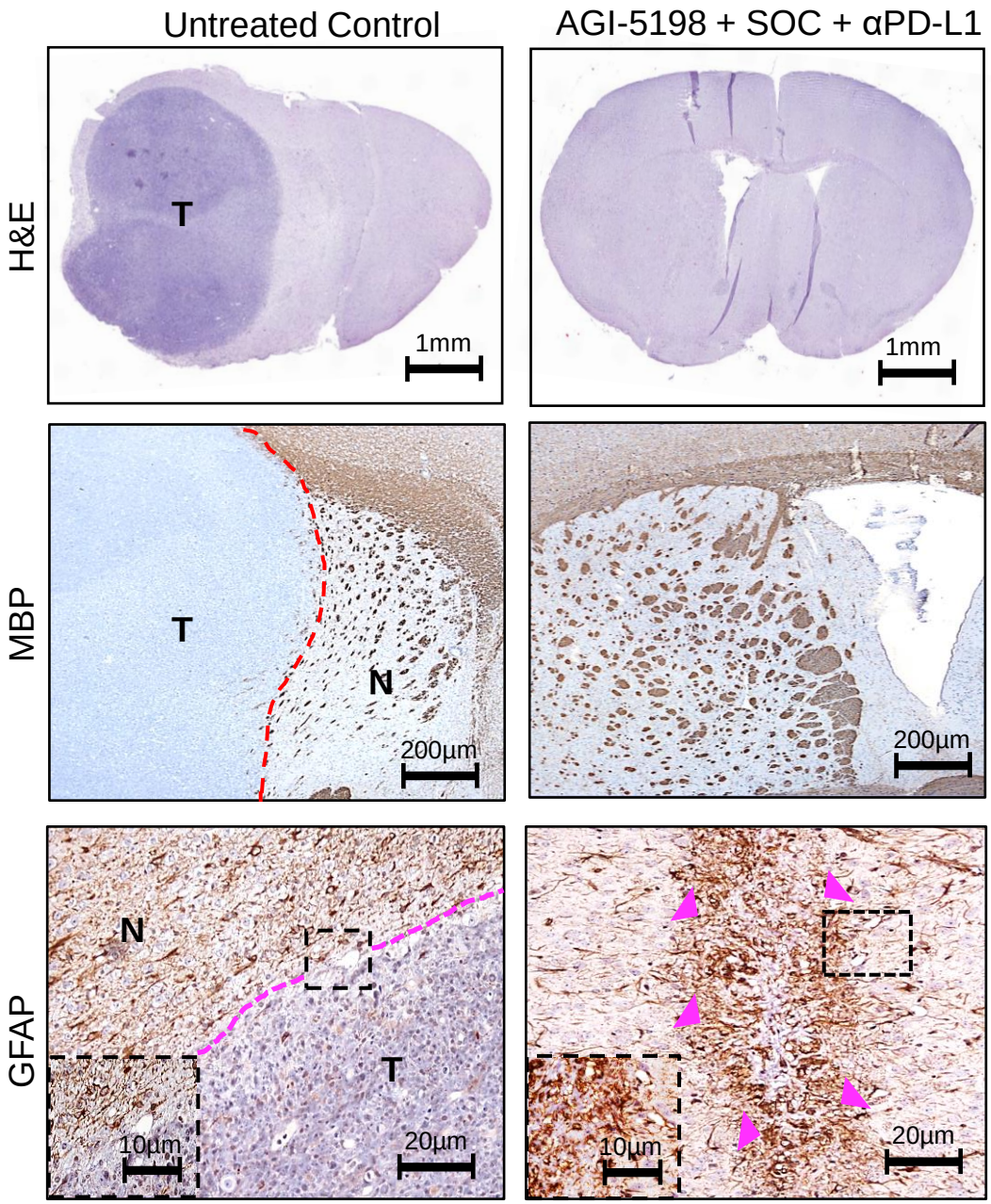

Supplementary Figure 15: Mutant IDH1 tumor bearing mice treated with IDH1-R132H inhibitor in combination with standard of care and anti-PDL1 immune checkpoint blockade show no evidence of histological alterations in the brain. Paraffin embedded 5µm brain sections were obtained from saline (30dpi), and long-term survivors in the AGI-5198+SOC+αPDL1 treatment groups (60dpi after rechallenge with mIDH1 NS). Brain sections from each treatment group were stained for hematoxylin and eosin (H&E), myelin basic protein (MBP) or Glial fibrillary acidic protein (GFAP). Pink arrows in the lower magnification panel for the GFAP staining show activated astrocytes in the vicinity of the scar tissue where the tumor was originally implanted. Normal brain = N and tumor tissue = T (representative image from *n* = 3 biological replicates).

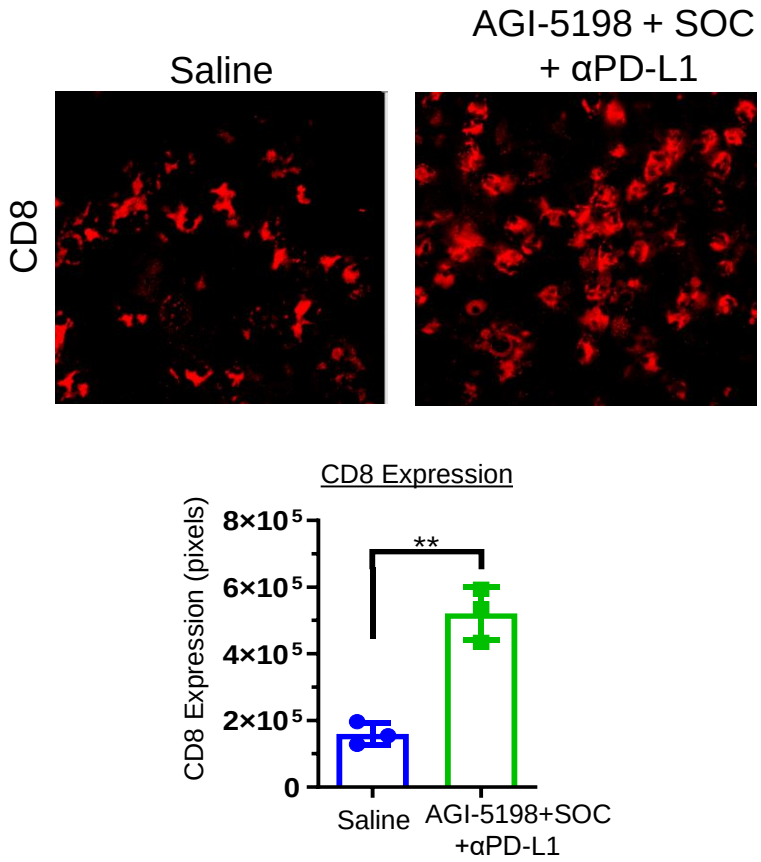

Supplementary Figure 16: CD8 Expression in mIDH1 bearing mice treated with IDH1-R123H inhibition, standard of care, and αPD-L1 immune checkpoint blockade. C57BL/6 mice bearing mIDH1 glioma were treated with saline or AGI-5198+SOC+αPD-L1 as detailed in Figure 4A. At 27 dpi, brains were harvested for immunohistochemistry analysis. Immunofluorescence staining for CD8 was performed on 50 µm vibratome tumor sections. Bar graphs represent total number of positive cells for CD8 in saline or AGI-5198+SOC+αPD-L1 treatment groups. $^{**}P < 0.01$; unpaired t-test. Bars represent mean ± SEM (n = 3 biological replicates).

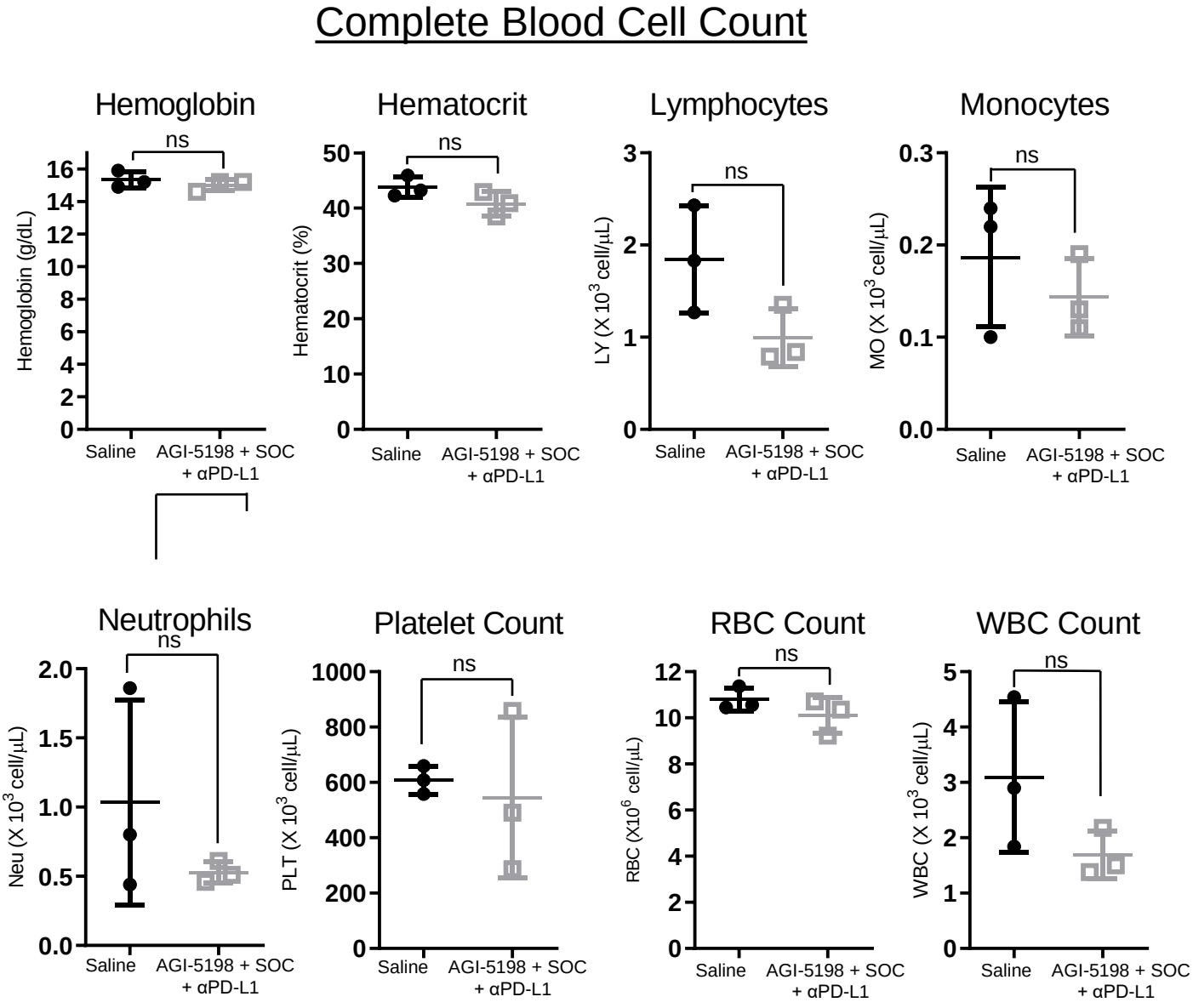

Supplementary Figure 17: Mutant IDH1 tumor bearing mice treated with IDH1-R132H inhibitor in combination with SOC and anti-PDL1 immune checkpoint blockade exhibit normal complete blood cell (CBC) counts. Blood was collected from mIDH1 tumor bearing mice treated with saline or AGI-5198 + SOC + αPD-L1 at 27 dpi. For each treatment group levels of hemoglobin, hematocrit, lymphocytes, monocytes, neutrophils, platelet count, and red blood cell (RBC) and white blood cell (WBC) counts were quantified. The counts between saline and AGI-5198 + SOC + αPD-L1 treatment groups were compared and were non-significant, $P > 0.05$ ($n = 3$ biological replicates).

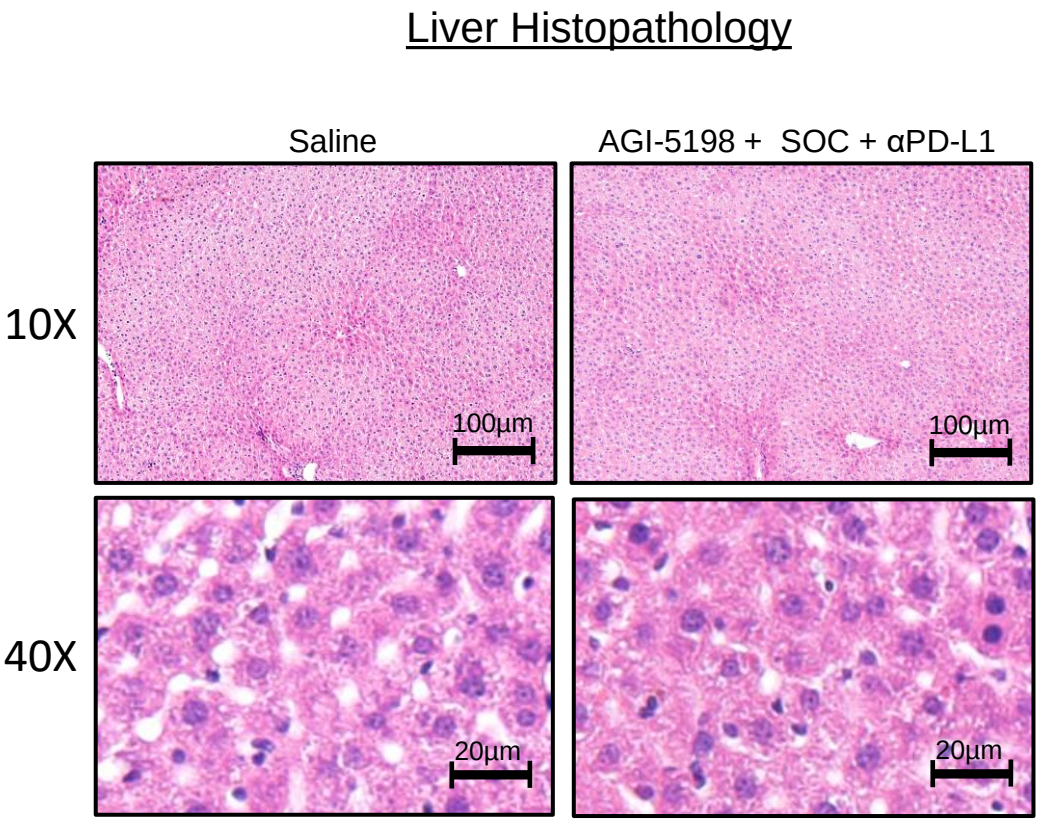

Supplementary Figure 18: Mutant IDH1 tumor bearing mice treated with IDH1-R132H inhibitor in combination with standard of care and anti-PDL1 immune checkpoint blockade show no evidence of histological alterations in the liver. H&E staining of paraffin embedded 5µm liver sections from mIDH1glioma bearing mice treated with saline or AGI-5198+SOC+αPD-L1 treatment groups at 27dpi. Low (10X) and high (40X) magnification images for each treatment condition are displayed (representative image from *n* = 3 biological replicates).

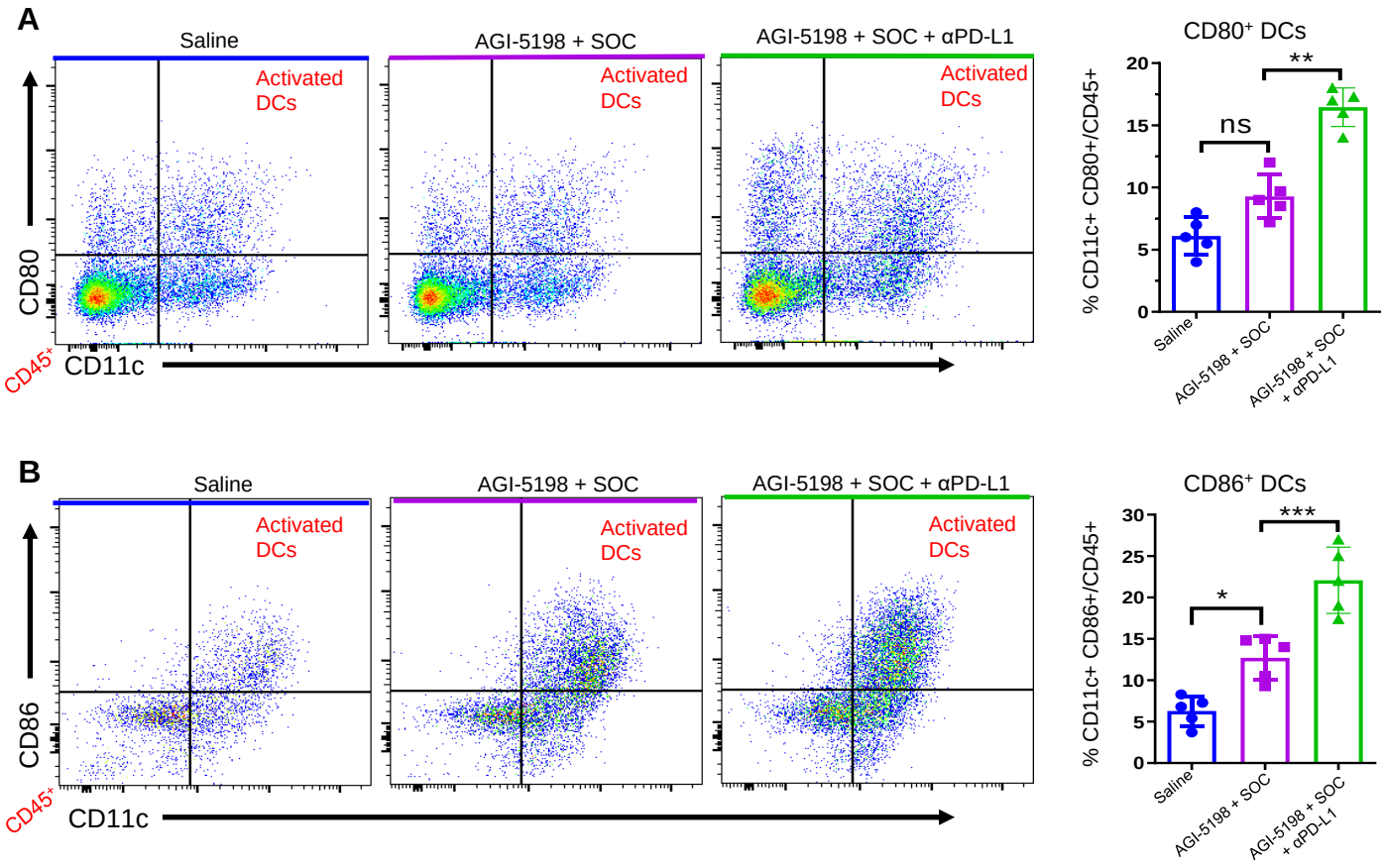

Supplementary Figure 19: **Inhibition of IDH1-R132H in combination with standard of care and anti-PDL1 blockade increases the infiltration of activated dendritic cells (DCs) in the mIDH1 glioma TME.** Quantification of the percent of activated (**A**) CD80 positive and (**B**) CD86 positive DCs in the TME of saline, AGI-5198+IR, or AGI-5198 + SOC + αPD-L1 treated mIDH1-OVA glioma bearing mice was assessed at 27 dpi. **P* < 0.05; ***P* < 0.001 one-way ANOVA test. Bars represent mean ± SEM (*n* = 5 biological replicates).

Supplementary Figure 20

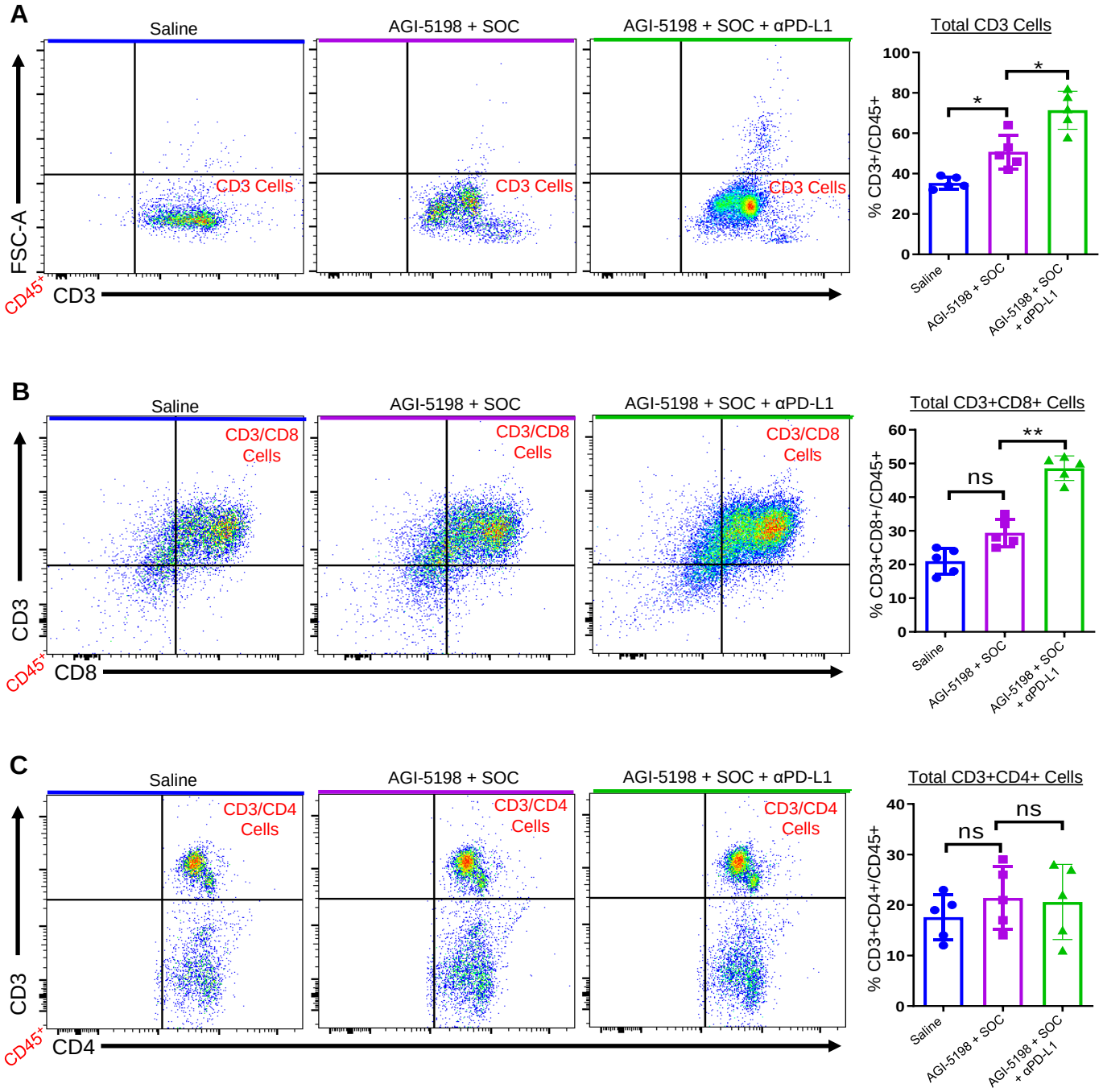

Supplementary Figure 20: **Inhibition of IDH1-R132H in combination with standard of care and anti-PDL1 blockade increases the infiltration of CD8+ T cells in the mIDH1 glioma TME.** Quantification of the percent of total (**A**) CD3, (**B**) CD3+/CD8+, or (**C**) CD3+/CD8+ T cells in the TME of saline, AGI-5198+IR, or AGI-5198+SOC+αPD-L1 treated mIDH1-OVA glioma bearing mice was assessed at 27 dpi. *$P < 0.05$; **$P < 0.001$; ns = non-significant; one-way ANOVA test. Bars represent mean ± SEM ($n = 5$ biological replicates).

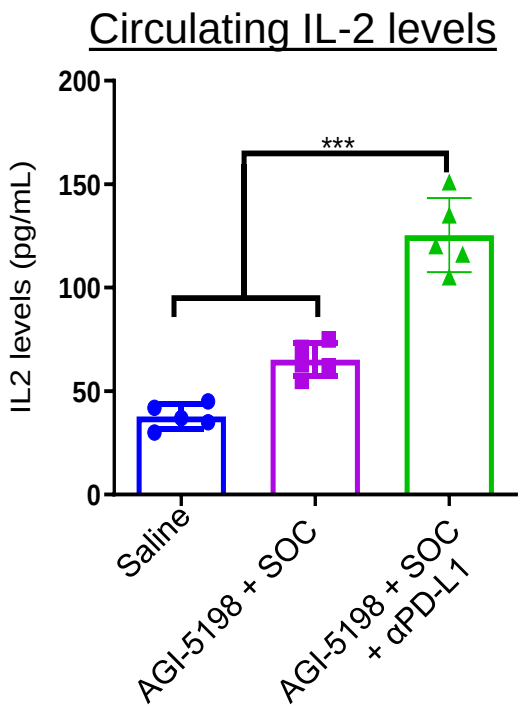

Supplementary Figure 21: The sera of mIDH1 tumor bearing mice treated with IDH1-R132H inhibitor in combination with standard of care and anti-PDL1 immune checkpoint blockade exhibit high levels of IL-2. (A) Quantification of IL2 in the sera of mIDH1-OVA tumor bearing mice after treatment with saline, AGI-5198 + IR, or AGI-5198 + SOC + αPD-L1 at 27 dpi. IL2 levels were assessed by ELISA. ***$P < 0.001$, one-way ANOVA test. Bars represent mean ± SEM (n = 5 biological replicates).

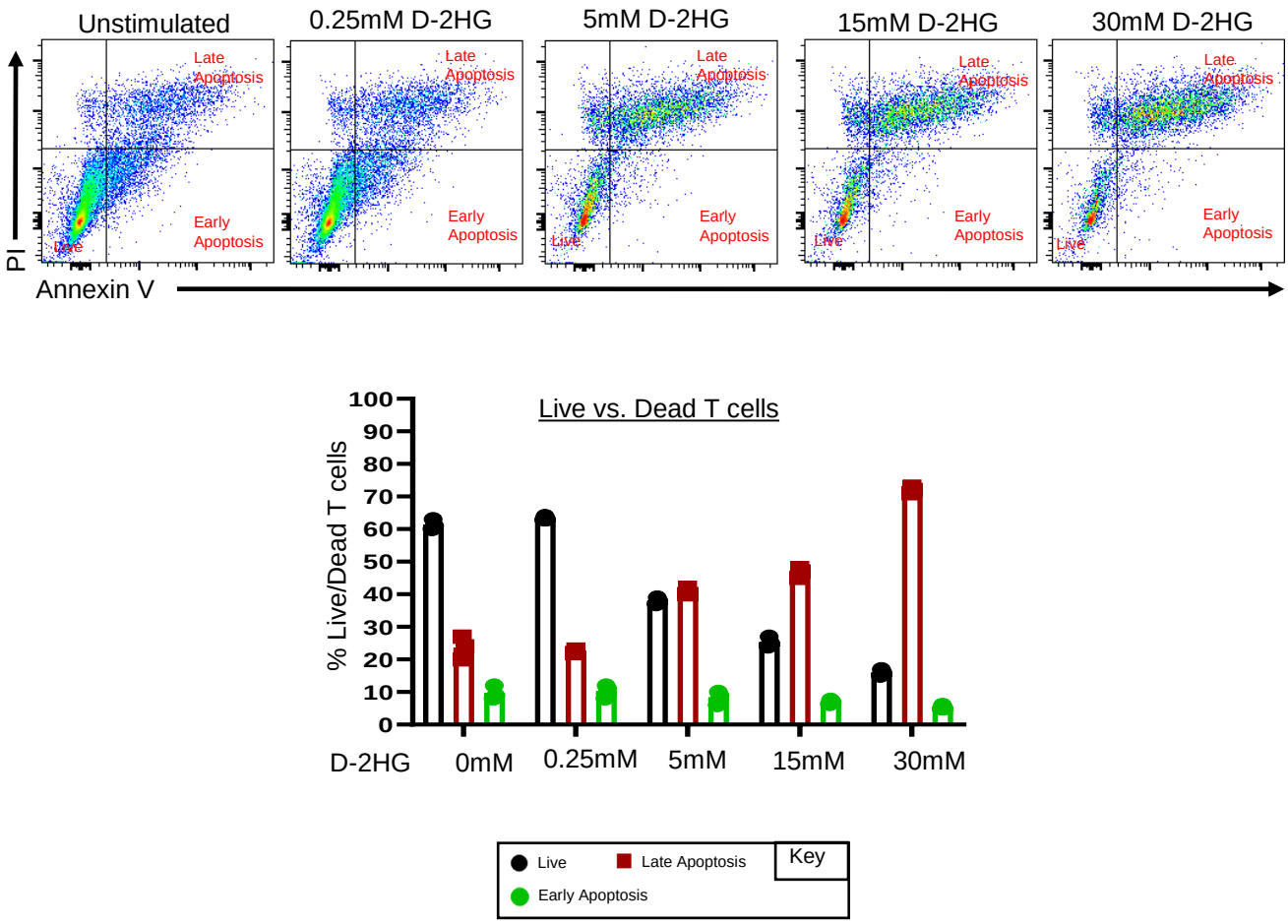

Supplementary Figure 22: D-2HG treatment induces T cell apoptosis. OT-1 splenocytes were incubated with 0.25mM, 5mM, 15mM or 30mM of D-2HG for 4 days. Then they were stained with Annexin V-FITC and propidium iodide (PI). Live non-activated T cells ($CD3^+/CD8^+$) were identified as Annexin V negative and PI negative. Dead T cells undergoing early apoptosis were identified as Annexin V positive and PI negative. Dead T cells undergoing late apoptosis were identified as Annexin V positive and PI positive. Bars represent quantitative analysis of the distribution of live and dead cells during 4-day incubation period with D-2HG (*n* = 3 technical replicates).

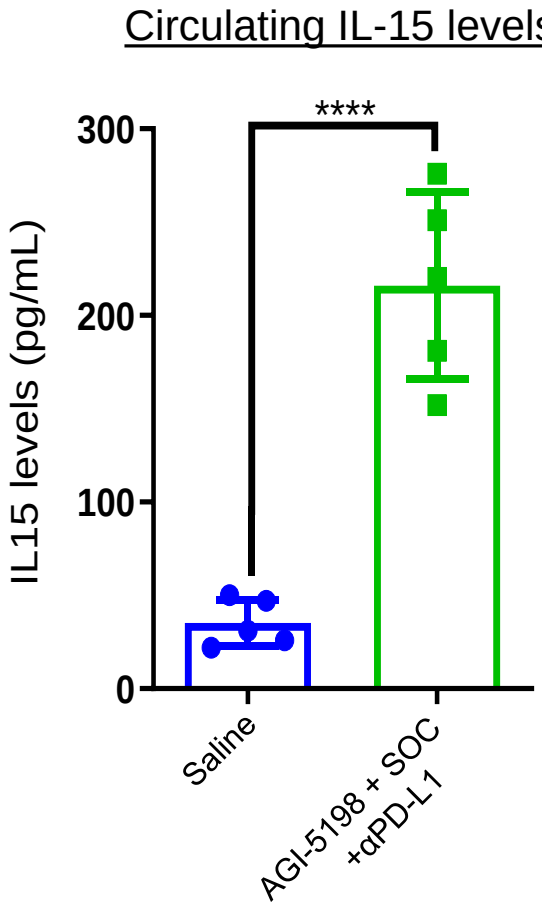

Supplementary Figure 23: The sera of long-term survivors from AGI-5198 + SOC + αPD-L1 treatment rechallenged with mIDH1 glioma exhibit high levels of IL-15. Long-term survivors from the AGI-5198 + SOC + αPD-L1 treatment group were rechallenged in the contralateral hemisphere with mIDH1 NS. As a control group, untreated normal mice were implanted with mIDH1 and did not receive further treatment. Sera were collected from mice at 14 dpi after rechallenge. Quantification of IL15 in the sera of untreated or rechallenged AGI-5198 + IR + TMZ + αPD-L1 mIDH1 tumor bearing mice. IL15 levels were assessed by ELISA. ****$P < 0.0001$, One-way ANOVA test. Bars represent mean ± SEM (n = 3 technical replicates).

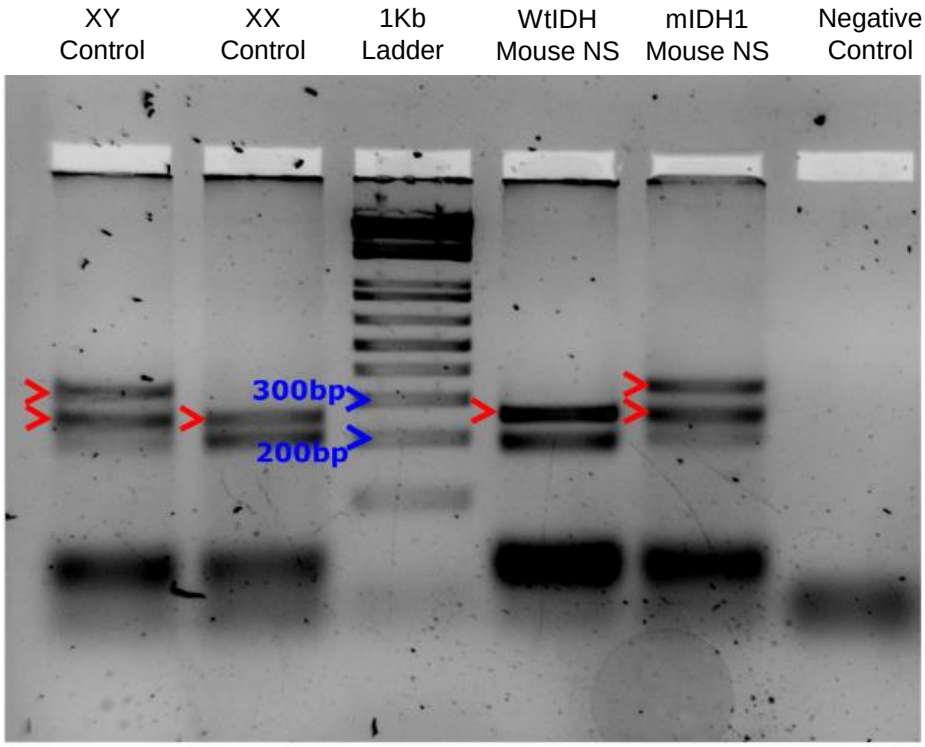

Supplementary Figure 24: Genetic sex determination of WtIDH and mIDH1 mouse-NS. Sex determination of mouse-NS was performed using simplex PCR. WtIDH mouse-NS display bands for XX genotype while the mIDH1 mouse-NS display bands for XY genotype. Genomic DNA extracted from blood of male and female C57BL6 mice, respectively were used as positive control for both genders. Expected bands: a 269 bp product from the X chromosome and a 353 bp product from the Y chromosome.

Supplementary Figure 25

Flowcytometry Gating Strategy

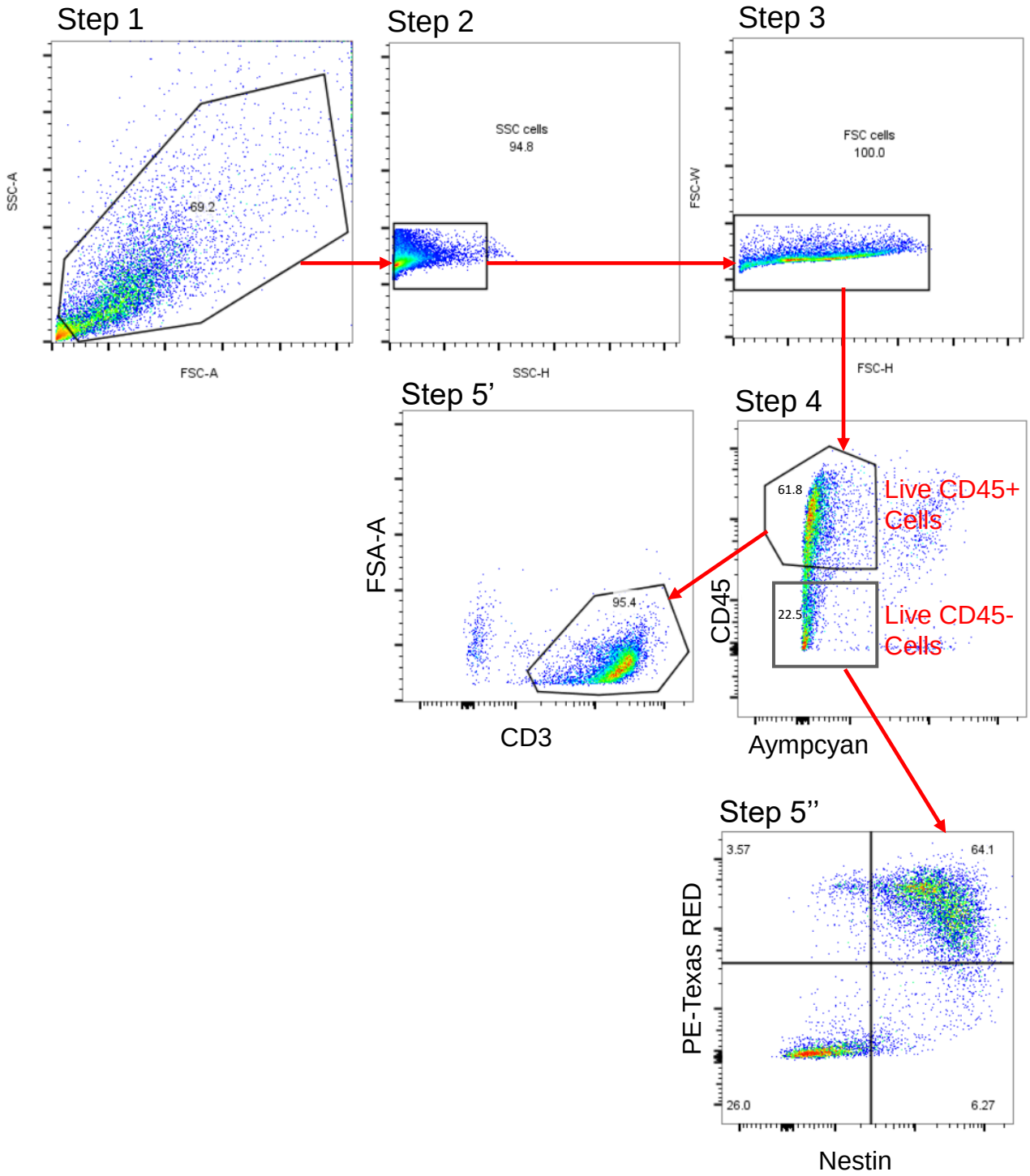

Supplementary Figure 25: Gating strategy used for flow cytometry analysis of tumor infiltrating and peripheral lymphocytes. Step 1: Immunolabeled lymphocytes were gated to exclude cellular debris. Step 2 and Step 3: Doublet discrimination gating was performed to filter out cellular aggregates prior to analysis. Step 4: CD45+/Aymcyan- gate to identify live mIDH1 glioma infiltrating immune cells. CD45-/Aymcyan- gate to identify tumor cells. Step 5': Identification of live CD3+ cells. Step 5: Identification of Katushka+/nestin+ live tumor cells.

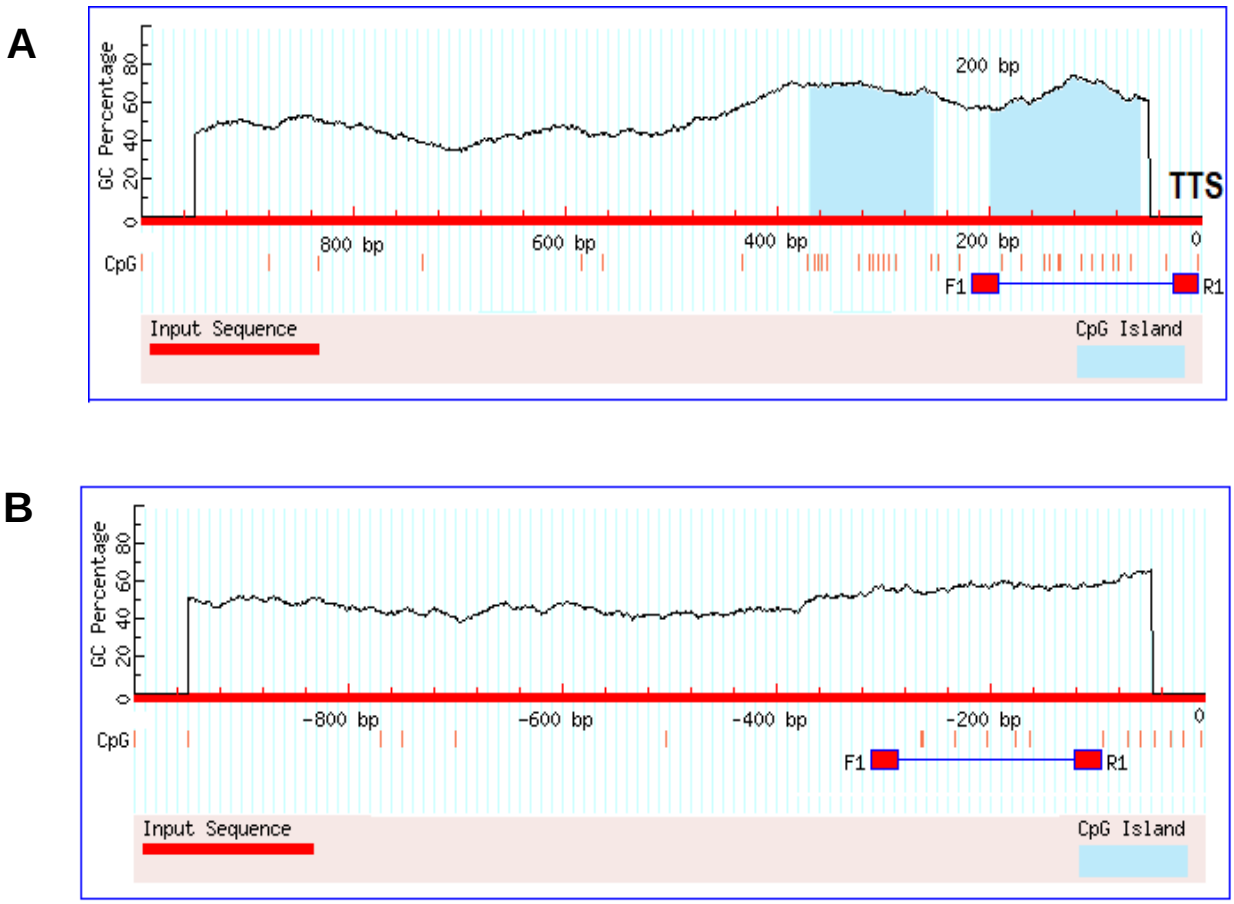

Supplementary Figure 26: **Identification of CpG elements downstream of PD-L1 or MGMT genes' transcription start site.** (**A**) CpG island identification in mouse PD-L1 gene promoter. F1 and R1 indicate the location of primers used. (**B**) CpG island identification in mouse MGMT gene promoter. F1 and R1 indicate the location of primers used.

Table 1: Log-rank (Mantel-Cox) Kaplan Meir Survival Analysis for AGI-5198 treatment in combination with IR

Group	P value
Saline (MS: 34d) vs. IR (MS:35d)	0.2538
Saline (MS: 34d) vs. AGI-5198 (MS: 43d)	0.0406
Saline (MS: 34d) vs. AGI5198 + IR (MS:50d)	<0.0001
AGI-5198 (MS: 43d) vs. AGI5198 + IR (MS:50d)	0.5818

Table 2: Log-rank (Mantel-Cox) Kaplan Meir Survival Analysis for AGI-5198 treatment in combination with SOC and αPD-L1 immune check point blockade

Group	P value
Saline (MS: 35d) vs. AGI-5198 + TMZ + αPD-L1 (MS:42d)	0.0686
Saline (MS: 35d) vs. AGI-5198 + SOC (MS: 52d)	0.0018
Saline (MS: 35d) vs. AGI5198 + IR + αPD-L1 (MS: 61d)	0.0018
Saline (MS: 35d) vs. AGI5198 + SOC + αPD-L1 (MS: undefined)	0.0018
AGI-5198 + TMZ + αPD-L1 (MS: 42d) vs. AGI-5198 + SOC (MS: 52d)	0.9331
AGI-5198 + TMZ + αPD-L1 (MS: 42d) vs. AGI5198 + IR + αPD-L1 (MS: 61d)	0.6013
AGI-5198 + TMZ + αPD-L1 (MS:42d) vs. AGI5198 + SOC + αPD-L1 (MS: undefined)	0.3386
AGI-5198 + SOC (MS: 52d) vs. AGI5198 + IR + αPD-L1 (MS: 61d)	0.3655
AGI-5198 + SOC (MS: 52d) vs. AGI5198 + SOC + αPD-L1 (MS: undefined)	0.1599
AGI5198 + IR + αPD-L1 (MS: 61d) vs. AGI5198 + SOC + αPD-L1 (MS: undefined	0.6943

Table 3: Log-rank (Mantel-Cox) Kaplan Meir Survival Analysis for AGI-5198 treatment in combination with SOC and αPD-L1 immune check point blockade

Group	P value
Saline (MS: 34d) vs. TMZ (MS:39d)	<0.01
IR (MS: 35d) vs. SOC (MS: 38d)	<0.01
AGI-5198 (MS: 43d) vs. SOC (MS: 38d)	<0.001
AGI-5198 (MS: 43d) vs aPD-L1 (MS: 39d)	<0.05
AGI-5198 (MS: 43d) vs TMZ (MS: 39d)	<0.05
AGI-5198 (MS: 43d) vs. AGI5198 + IR (MS:50d)	0.5818
AGI-5198 + SOC (MS: 52d) vs. AGI5198 + SOC + αPD-L1 (MS: undefined)	0.1599

Table 4: Long-Term survivors in AGI-5198 treatment in combination with SOC, IR, TMZ, and αPD-L1 immune check point blockade

Group	Percent of Long Term Survivors
IR	0%
TMZ	0%
aPD-L1	0%
AGI-5198	40%
AGI-5198 + IR	40%
AGI-5198 + SOC	20%
AGI-5198 + IR + aPD-L1	40%
AGI-5198 + TMZ + aPD-L1	40%
AGI-5198 + SOC + aPD-L1	60%

Table 5: Mice serum levels of biochemical variables after intraperitoneal treatment with AGI-5198 + IR+ TMZ + αPDL1 (n=3).

Group	Creatinine (µmol/L)	BUN (mmol/L)	ALT (U/L)	AST (U/L)
Saline	0.11 ± 0.17	30 ± 1.7	73 ± 7.2	303 ± 290.6
AGI5198 + IR+TMZ+ αPDL1	0.21 ± 0.02	19.3 ± 6.7	112.3 ± 31	311 ± 213.6

Table 6. Flowcytometry Antibodies

Antibodies	Source	Catalog Number
V450 rat anti mouse CD45 (clone: 30-F11), Flow 1:200	BD Bioscience	Cat# 560501
PE Rat anti mouse F4/80 (clone: BM8), Flow 1:200	Biolegend	Cat# 123110
Alexa Fluor 700 Rat anti mouse CD206 (clone: C068C2), Flow 1:200	Biolegend	Cat# 141733
PE armenian hamster anti mouse CD11c (clone: N418), Flow 1:200	Biolegend	Cat#117308
PercpCy5.5 rat anti mouse B220 (clone: RA36B2), Flow 1:200	Biolegend	Cat #: 103236
FITC rat anti mouse CD8 (clone: KT15) , Flow 1:1:00	Thermofisher	Cat # MA5-16759
PercpCy5.5 armenian hamster anti mouse CD3 (clone: 145-2C11), Flow 1:200	Biolegend	Cat # 100328
FITC rat anti mouse Gr-1 (clone: RB6-8C5), Flow 1:200	Biolegend	Cat # 108405
PercpCy5.5 rat anti mouse CD11b (clone: M1/70), Flow 1:200	Biolegend	Cat # 101230
FITC rat anti mouse CD4 (clone:GK1.5) , Flow 1:200	Biolegend	Cat # 100405
APC rat anti mouse CD25 (clone: 3C7), Flow 1:200	Biolegend	Cat # 101909
APC rat anti mouse CD44 (clone: IM7), Flow 1:200	Biolegend	Cat #: 103012
APC/Cy rat anti mouse CD62L (clone: MEL-14), Flow 1:200	Biolegend	Cat #: 104428
PE rat anti mouse IFNγ (clone: XMG1.2), Flow 1:200	Biolegend	Cat #: 505808
PE rat anti mouse PD-L1 (clone: B7-H1), Flow 1:200	Biolegend	Cat #: 124308
APC/Cy rat anti mouse PD-1 (clone: 29F.1A12), Flow 1:200	Biolegend	Cat #: 135224
APC rat anti mouse TIM 3 (clone: B8.2C12), Flow 1:200	Biolegend	Cat #: 134008
PE anti mouse TIGT(clone: 1G9), Flow 1:200	Biolegend	Cat #: 142104
PE/Cy7 armanian hamster anti mouse CD80 (clone: 16-10A1), Flow 1:200	Biolegend	Cat #: 104734
APC/Cy anti mouse CD86 (clone: GL-1), Flow 1:200	Biolegend	Cat #: 105030
FITC anti mouse MHC II (clone: 39-10-8) , Flow 1:200	Biolegend	Cat #: 115006
FITC rat anti mouse Foxp3 (clone MF-14), Flow 1:200	Biolegend	Cat # 126403
PE-Tetramer, Flow 1:100	MBL International	Cat # TB-5001-1
Alexa Fluor 647 rabbit anti mouse Calreticulin (clone: EPR3924) , Flow 1:50	Abcam	Cat # ab196159
Alexa Fluor 647 rabbit ant mouse pH3Ser10 (clone: D2C8), Flow 1:50	Cell Signaling	Cat # 3458S
Efluor 780-Live/Dead, Flow 1:200	Affymetrics	Cat #: 65-0865-14
Annexin V/PI Apoptosis Kit	Thermofisher	Cat #: V13241
Click-iT EdU Kit	Thermofisher	Cat #: C10418
Mouse Foxp3 Buffer Set	BD Biosciences	Cat #: 560409
BD CytoFix/Cytoperm Kit	BD Biosciences	Cat #: 554714

Table 7. Immunohistochemistry and Western Primary Antibodies

Antibodies	Source	Catalog Number
Rat anti mouse MBP, IHC 1:300	Millipore	Cat# MAB386
Rabbit anti mouse CD8, IHC: 1: 2000	Cedarlane	Cat #: 361003
Rat anti mouse GFAP, IHC: 1:1000	Millipore	Cat #: AB5541
Rabbit anti mouse Cleaved Caspase 3, IHC: 1:1000	Sell Signaling	Cat # 9661S
Rabbit anti mouse Ki-67	Abcam	Cat # ab15580
Rabbit anti mouse PD-L1	Cell Signaling	Cat # 13684T
Rabbit anti mouse/human LC3B I/II	Cell Signaling	Cat # 2775S
Rabbit anti mouse vinculin	Thermofisher	Cat # 700062
Mouse anti human β-actin	Sigma	Cat # 1978

Table 8. Immunohistochemistry and Western Secondary Antibodies

Antibodies	Source	Catalog Number
Goat polyclonal anti-rabbit biotin-conjugated, IHC 1:1000	Dako	Cat# E0432
Goat polyclonal anti-rat Alexa Fluor 594, IHC 1:1000	Thermo Fisher Scientific	Cat# A-11007
Goat polyclonal anti-rabbit biotin-conjugated, IHC 1:1000	Thermo Fisher Scientifc	Cat #: 31830
Goat polyclonal anti-rabbit Alexa Fluor 594, IHC 1:1000	Thermo Fisher Scientific	Cat#: A-32740
Goat polyclonal anti-rabbit HRP WB 1: 4000	Dako	Cat#: P0448
Goat polyclonal anti-mouse HRP WB 1:4000	Dako	Cat# P044701-2

Table 9. Reagents for In vivo Studies

Reagent	Source	Catalog Number
Polyethylene Glycol 400	Sigma-Aldrich	Cat#: 8170035000
AGI-5198	Amatek Chemicals	Cat#:1355326-35-0
Temozolomide	Selleckchem	Cat #: S1237
Rat Anti-mouse PD-L1	BioXcell	Cat# BE0101
Ethanol	Sigma-Aldrich	Cat #: 459836

Table 10. Primer Sequences

Primer Name	TARGET	Sequence (5' -> 3')
PD-L1_ms_R	Mouse PD-L1 promoter	GGT TGG AAT TTG CGG TTC TG
PD-L1_ms_L		CAG GAT TGG TTG GCT ATG AC
MGMT_ms_R	Mouse MGMT promoter	CTG GGT GCG TGT TCC TAG AG
MGMT_ms_L		CTCAGCGGGTAAACTGGGAC
PD-L1_hu_R	Human PD-L1 promoter	TCC TAG GAC ACC AAC ACT AGA TAC CTA AAC
PD-L1_hu_L		TCT GCC CAA GGC AGC AA